AD-A087 042 TEXAS A AND M UNIV COLLEGE STATION DEPT OF AEROSPACE--ETC F/G 20/11
THE PREDICTION OF RESPONSE OF SOLIDS TO THERMAL LOADING USING T--ETC(U)
MAY 80 D H ALLEN, W E HAISLER N00014-76-C-0150
UNCLASSIFIED TR-3275-80-1 NL

END
DATE FILMED
9-80
DTIC

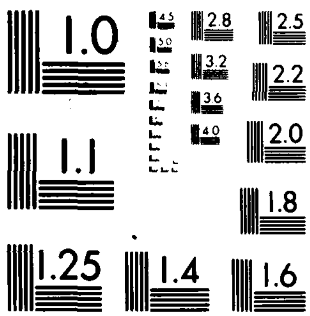

MICROCOPY RESOLUTION TEST CHART
NATIONAL BUREAU OF STANDARDS 1963 A

LEVEL II

THE PREDICTION OF RESPONSE OF SOLIDS TO THERMAL LOADING USING THE FINITE ELEMENT CODE AGGIE I

aerospace
engineering
department

TEXAS A&M UNIVERSITY

DAVID H. ALLEN AND WALTER E. HAISLER

OFFICE OF NAVAL RESEARCH
DEPARTMENT OF THE NAVY
WASHINGTON, D.C. 20025
CONTRACT NO. N00014 [illegible] C-0150
TASK [illegible]

TECHNICAL REPORT [illegible]

MAY 30, 1980

[illegible] ERING EXPERIMENT STATION

015

7

6 THE PREDICTION OF RESPONSE OF SOLIDS TO THERMAL LOADING USING THE FINITE ELEMENT CODE AGGIE I.

10 David H./Allen [redacted] Walter E./Haisler

Aerospace Engineering Department
Texas A&M University
College Station, Texas 77843

Office of Naval Research
Department of the Navy
Washington, D.C. 20025

15 N00014-78- - 0150

Contract No. N00014-C-0150

Task No. NR 064-534

14 TR-

9 Technical Report No. 3275-80-1

11 30 May [redacted]80

12 53

404277

The Prediction of Response of Solids to Thermal Loading Using the Finite Element Code AGGIE I

David H. Allen* and Walter E. Haisler**

ABSTRACT

In previous work the authors have proposed a theory for predicting the response of elastic-plastic solids subjected to thermal loads. The theory was cast in a finite element framework and has now been placed in the finite element code AGGIE I. In this paper several example problems will be compared to experimental and other theoretical results. It will be shown that the model in its current form is adequate for modelling the response of many solids composed of temperature dependent materials.

INTRODUCTION

In our latest two reports[1,2] we proposed a constitutive law for predicting the response of elastic-plastic-creep materials to thermal load histories. It will be recalled that the incremental theory of plasticity was used to obtain a constitutive law of the form

$$dS_{ij} = C^{t}_{ijmn}\ (dE_{mn} - dE^{C}_{mn} - dE^{T}_{mn}) + dP_{ij}, \qquad (1)$$

where dS_{ij} is the stress increment tensor,

C^{t}_{ijmn} is the effective modulus tensor,

*Research Assistant, Aerospace Engineering Department, Texas A&M University, College Station, Texas 77843

**Associate Professor, Aerospace Engineering, Texas A&M University, College Station, Texas 77843

dE_{mn} is the total strain increment tensor,

dE^C_{mn} is the creep strain increment tensor,

dE^T_{mn} is the thermal strain increment tensor, and

dP_{ij} is the stress increment tensor caused solely by a change in material properties due to a temperature change during the load step. The constitutive law employed the combined isotropic-kinematic hardening rule in order to model the Bauschinger effect in metals during cyclic loading. The resulting theory is similar in some respects to theories proposed by others, most notably Snyder and Bathe,[3] and Yamada and Sakurai.[4]

In our previous papers the constitutive law was also emplaced in an incremental variational principle and the finite element method was then used to discretize the equations of motion into a set of algebraic equations. The resulting theory was then applied to the finite strain finite element code AGGIE I.[5] This code uses the two dimensional isoparametric element proposed by Zienkiewicz[6] to model both material and geometrically nonlinear response.

The purpose of this paper is to verify that the code is now in operational form. This will be accomplished first by reviewing significant aspects of the code, and second by presenting the results of several example problems. It will be shown that not only does the code give quite accurate results in predicting many real world phenomena, but that this theory is both correct and computationally superior to that proposed by others. Finally, some significant shortcomings of the theory will be exposed for further research.

SIGNIFICANT ASPECTS OF THE CODE

There are several special cases encompassed withing equation (1). These cases are distinguished by the nature of the response of the medium as well as required input data and computation time. Accordingly, we have constructed four separate material models within the code as a means of affording maximum economy. The first model we have defined is quasi-isothermal elastic, where quasi-isothermal is defined to mean that the medium may undergo thermal loading, but that material properties are not significantly altered due to the temperature change. Under these conditions equation (1) reduces to

$$dS_{ij} = D_{ijmn}\ (dE_{mn} - dE^{C}_{mn} - dE^{T}_{mn}), \tag{2}$$

where D_{ijmn} is the elastic constitutive tensor. The second model is named nonisothermal elastic and differs from model one in that the thermal loading is such that material propertie must be considered to be a function of temperature. In this case equation (1) reduces to

$$dS_{ij} = D^{t+\Delta t}_{ijmn}\ (dE_{mn} - dE^{C}_{mn} - dE^{T}_{mn}) + dD_{ijmn}\ (E^{t}_{mn} - E^{Ct}_{mn} - E^{Tt}_{mn}) \tag{3}$$

where $D^{t+\Delta t}_{ijmn}$ is the elastic constitutive tensor at the end of the load step, dD_{ijmn} is the increment in the elastic constitutive tensor during the load step due to temperature change, and superscripts denote quantities evaluated at the start of the load step. In the third model the material is allowed to yield, but material properties are assumed to be independent of temperature. This model is appropriately named quasi-isothermal elastic-plastic, and equation (1) reduces under these assumptions to

$$dS_{ij} = C_{ijmn} (dE_{mn} - dE^C_{mn} - dE^T_{mn}). \qquad (4)$$

The final model, called nonisothermal elastic-plastic, incorporates no simplifying assumptions in the theory and accordingly is given by equation (1). These four models comprise the temperature dependent modelling capability of the code AGGIE I.

There are several nuances within the code which should be outlined before proceeding with example problems. First, one will recall that in order to solve the thermal stress problem one must characterize the temperature distribution within the medium. In its present configuration the code AGGIE I does not have this capability. It is assumed that the heat transfer solution is known a priori. The temperature distribution is input to the code by specifying nodal temperatures and utilizing the serendipity functions employed in the isoparametric element to interpolate within elements. It should also be pointed out that although creep can be predicted utilizing an uncoupled creep strain term, the emphasis in this paper will be on plasticity and thermal effects. Thus, most example problems included herein will have negligible creep.

The required input material data will depend on the model being used. For example, for the nonisothermal elastic-plastic model it is necessary to input a set of isothermal stress-strain curves at varying temperatures, as well as curves giving Poisson's ratio and the coefficient of thermal expansion as well as functions of temperature.[2]

EXAMPLE PROBLEMS

The example problems included herein have been chosen primarily as verification of each of the different models within the code AGGIE I.

The object of these examples is threefold in nature: (1) to verify the accuracy of the constitutive theory for modelling some nonlinear phenomena, (2) to support the claim that the constitutive theory has been correctly emplaced in the finite element code AGGIE I, and (3) to familiarize potential code users with the modelling capability of AGGIE I. These examples are presented here in ascending order of complexity.

I. Pseudo-Isothermal Static Elastic Circular Disk with Radial Temperature Variation

The first problem is that of a circular disk which undergoes a radial temperature change as shown in Figure 1. The temperature change is assumed to be small enough that response is elastic and material properties are not temperature dependent. The problem is solved in a single step using the two dimensional isoparametric element mesh shown in Figure 1. Although this problem may be solved more efficiently with an axisymmetric theory, the analysis is performed here assuming plane stress (Figure 2) and plane strain (Figure 3) conditions. Shown in the figures are comparisons for the radial displacement v, the radial normal stress σ_{rr}, and the circumferential normal or hoop stress $\sigma_{\theta\theta}$. In the figures it is seen that the results obtained in AGGIE I agree quite well with the theoretical solution reported by Boley and Weiner.[7] This is intended to verify the supposition that the pseudo-isothermal elastic constitutive law within the code is correct for plane stress and plane strain analysis.

II. Pseudo-Isothermal Static Elastic Axisymmetric Shell with Slow Heat Input

In the second problem the spherical cap shown in Figure 4 is subjected to an internal pressure of 100 PSI and a slowly applied heat input on the outer surface such that the temperature on the outer surface is $100^{\circ}F$ with

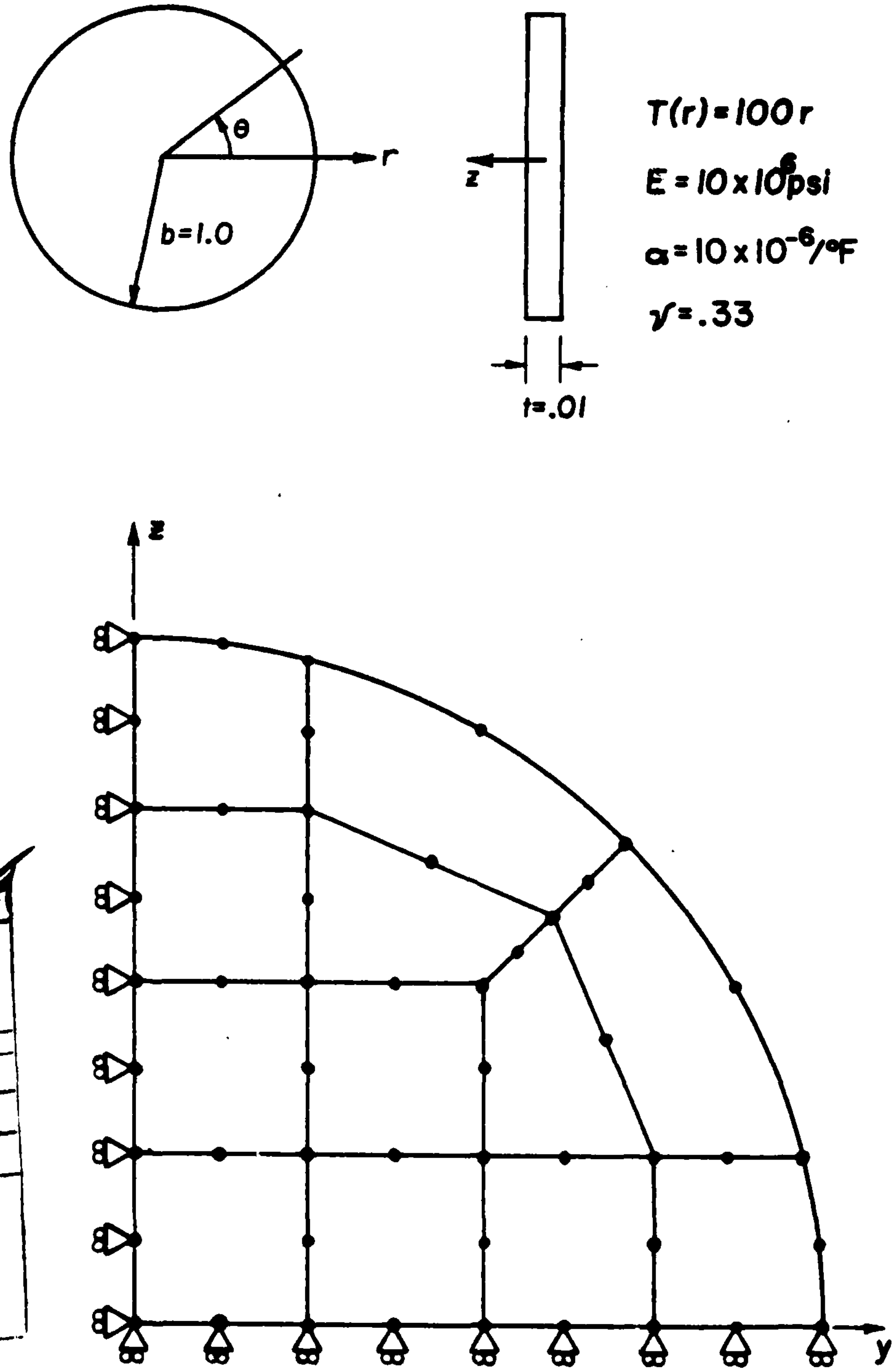

Figure 1. Geometry and Input Data for Example One

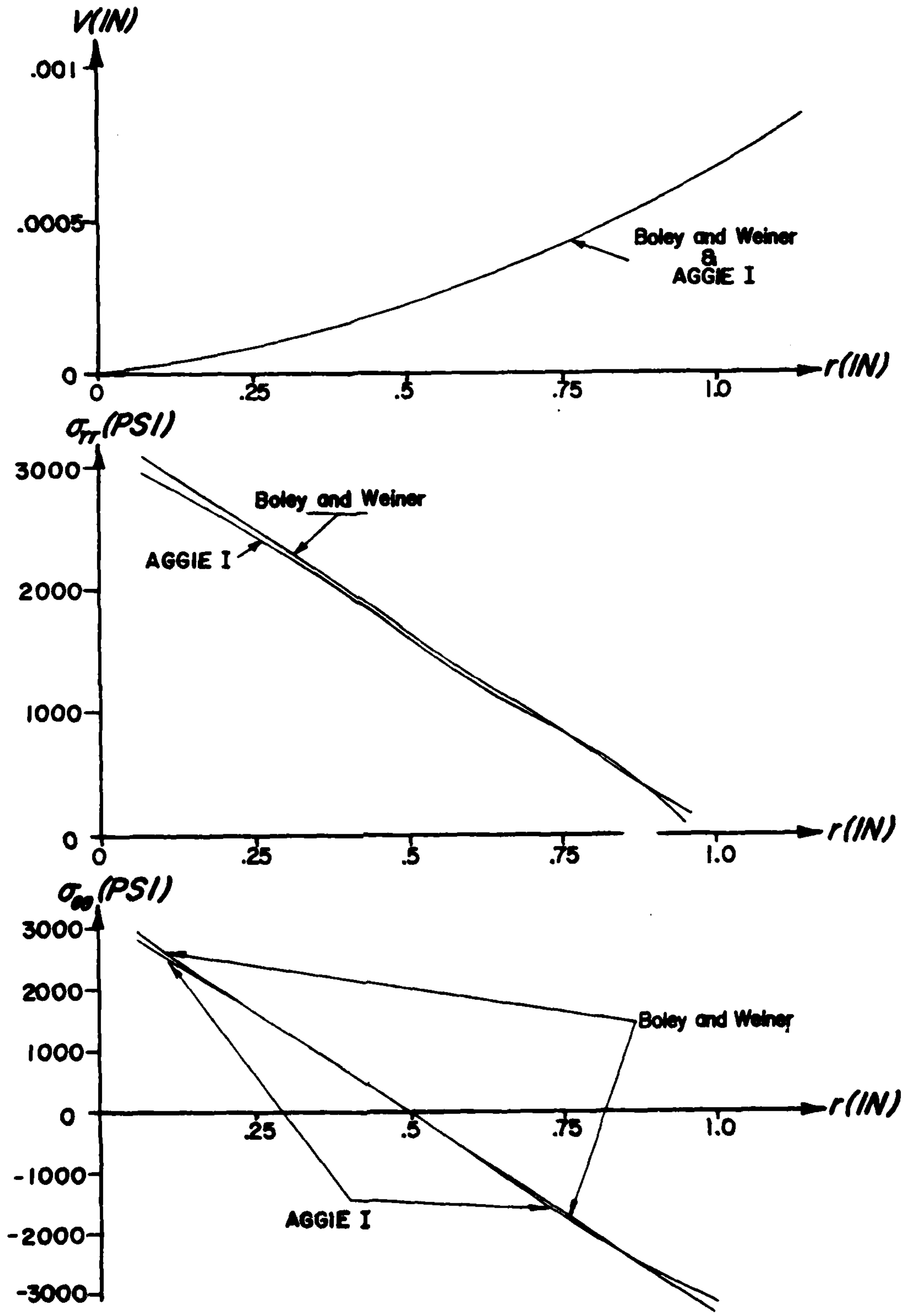

Figure 2. Analysis of Example One in Plane Stress Condition

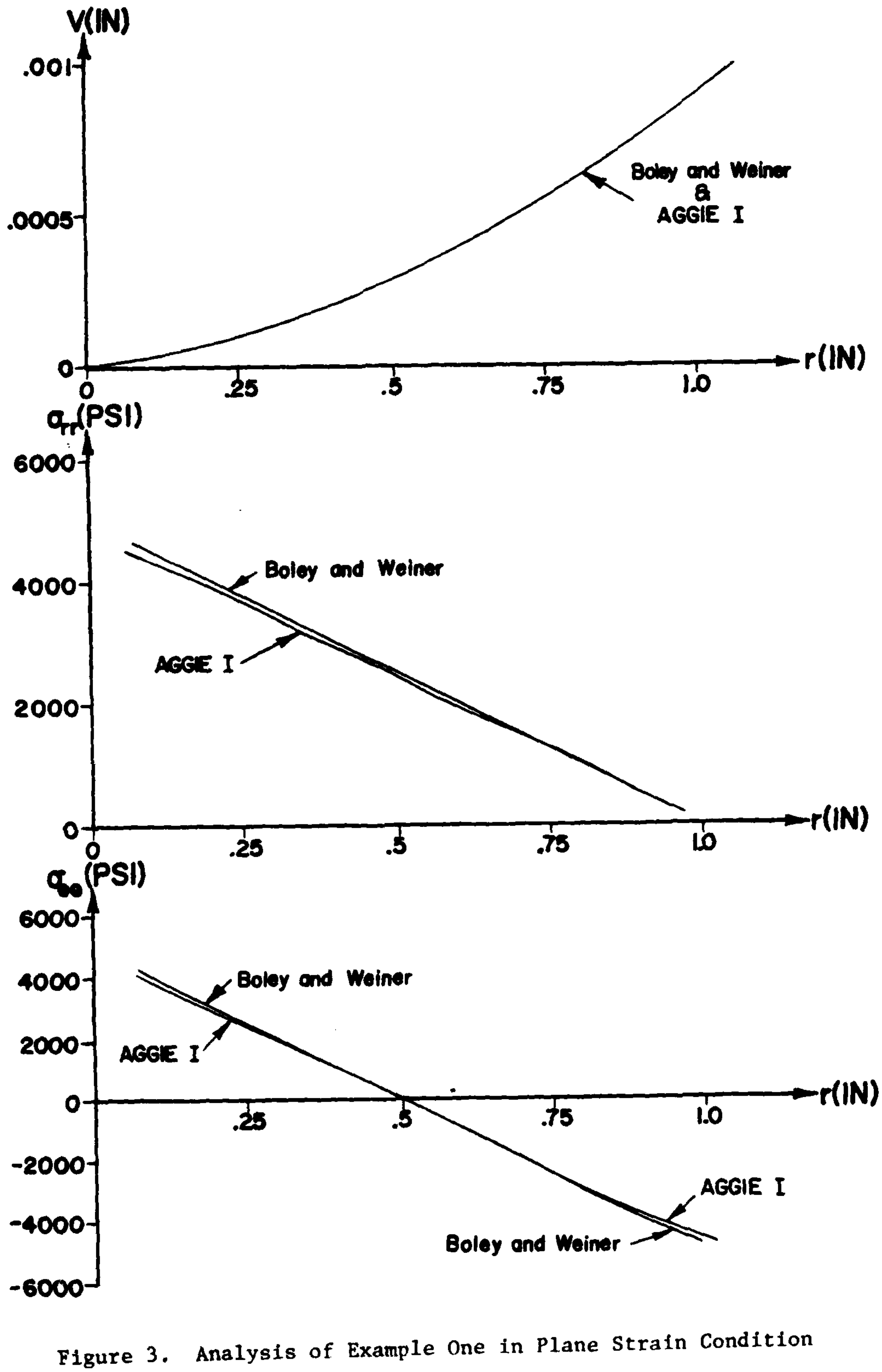

Figure 3. Analysis of Example One in Plane Strain Condition

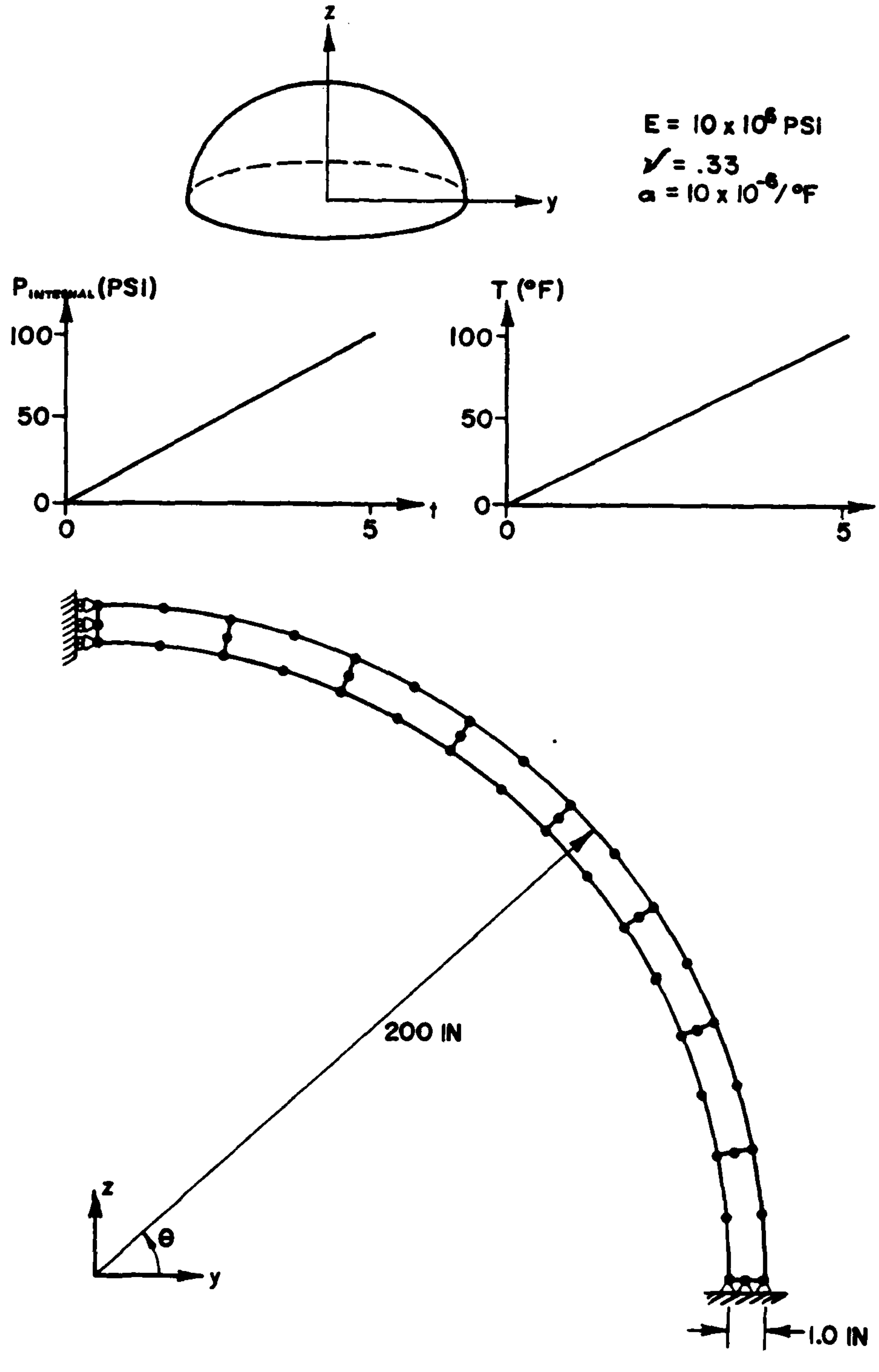

Figure 4. Geometry and Input Data for Example Two

a linear through thickness variation to $0^{\circ}F$ on the inner surface. The problem has been solved using axisymmetric analysis with the finite element grid shown in Figure 4. The resulting vertical (w) and horizontal (v) deflections are plotted in Figure 5 and compared to results obtained with the shell codes SAMMSOR[8] and SNASOR.[9] It is seen that good agreement is obtained between the analyses, and thus it is assumed that the code gives accurate results when using axisymmetric analysis in conjunction with the elastic pseudo-isothermal constitutive law.

III. Pseudo-Isothermal Dynamic Elastic Cantilever Beam with Rapid Heat Input

In this example the simply supported elastic beam shown in Figure 6 undergoes free vibration when subjected to a rapidly applied heat input on the upper surface. The heat transfer problem is assumed to be uncoupled from the deformation analysis, and thus the temperature distribution has been obtained from Boley and Weiner.[7] Using dynamic analysis and the finite element mesh shown in Figure 6 the neutral axis deflection at the center of the beam has been determined and compared to the theoretical analysis obtained by Boley and Weiner[7] in Figure 7. In addition, the results shown herein have been obtained by Snyder and Bathe.[3] It is seen that the dynamic capability of the program is confirmed for this material law.

IV. Nonisothermal Elastic Axial Bar Subjected to Simultaneous Mechanical Load and Heat Input

The fourth example demonstrates the capability of the code to predict the static response of elastic materials with strongly temperature dependent material properties to simultaneous mechanical and thermal loading. A significant factor in the accuracy of the theory is the correct deter-

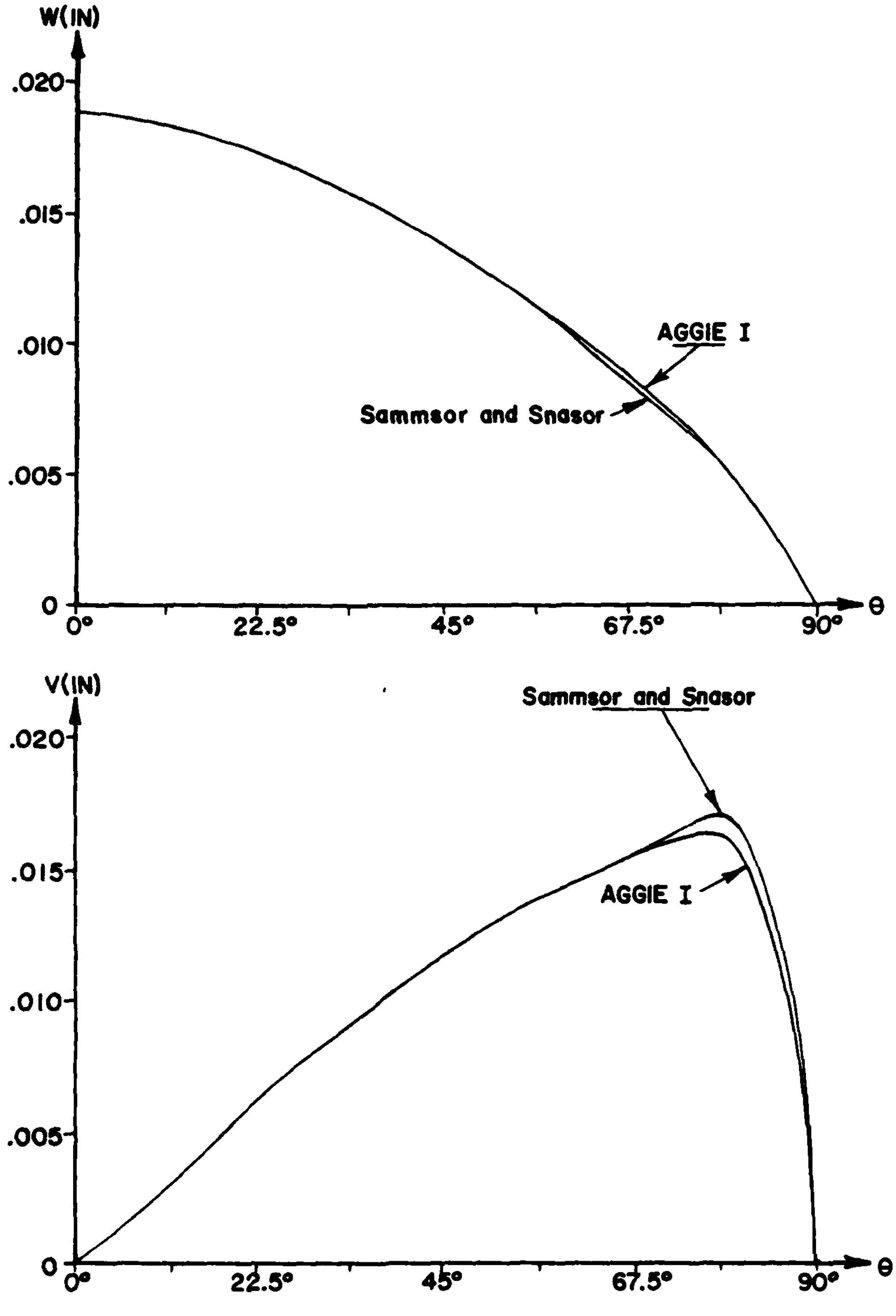

Figure 5. Computer Code Comparison for Analysis of Example Two

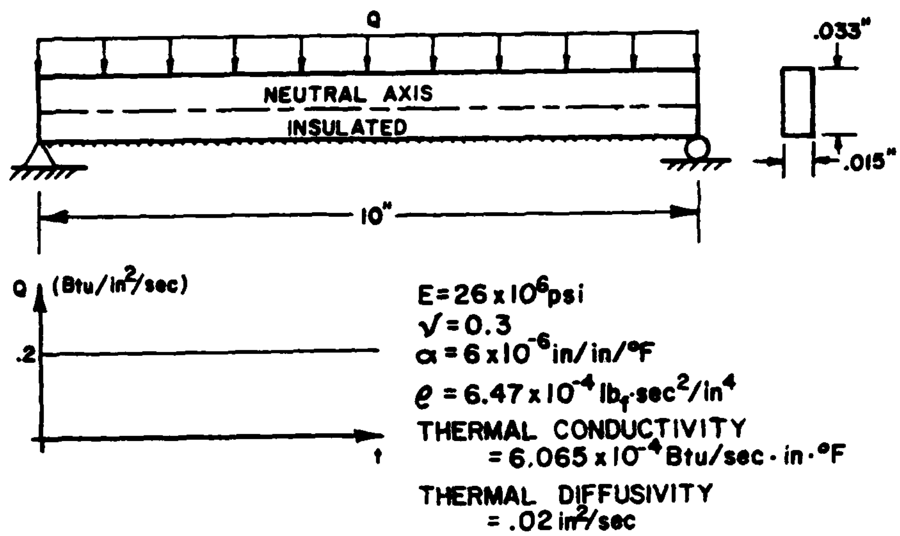

SIMPLY SUPPORTED BEAM AND HEAT INPUT

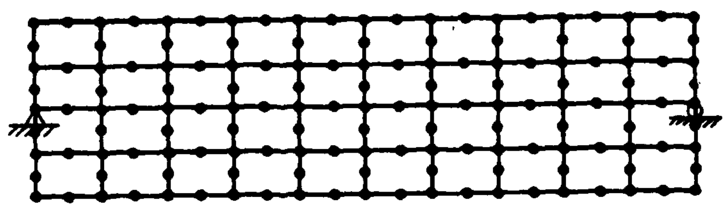

FINITE ELEMENT MESH, FORTY 8 NODE ELEMENTS

Figure 6. Input and Material Properties for Example Three

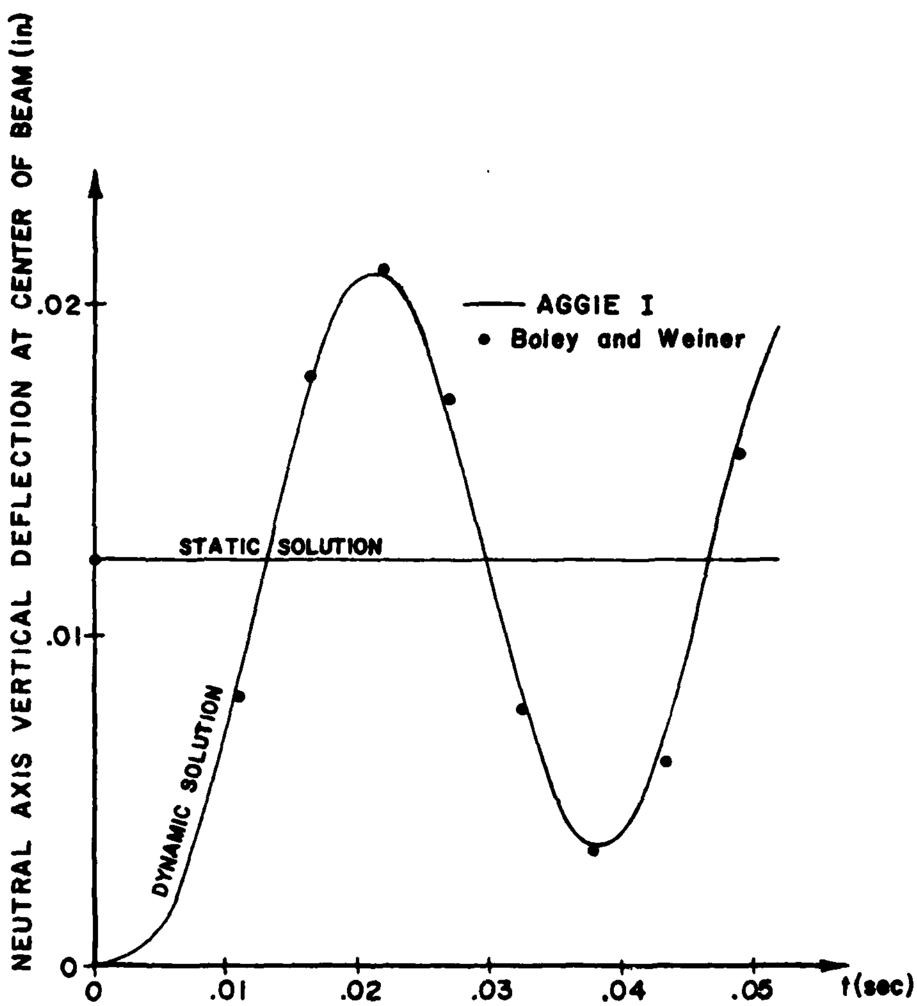

Figure 7. Comparison of Results for Example Three

mination of the thermal strain increment during a nonisothermal load step. To support this statement a theoretical discussion will be included in this example and this theory will be verified by experimental verification.

First, consider the elastic stress increment equation, which has been previously determined[1] to be represented by equation (3)

$$dS_{ij} = D_{ijmn}^{t+\Delta t} \left(dE_{mn} - dE_{mn}^{T}\right) + dD_{ijmn} \left(E_{mn}^{t} - E_{mn}^{Tt}\right) . \tag{5}$$

In order to determine the correct definition of dE_{mn}^{T} in this equation, consider a uniaxial case with no creep. Equation (3) thus reduces to

$$d\sigma = E^{t+\Delta t} \left(d\varepsilon - d\varepsilon^{T}\right) + dE \left(\varepsilon^{T} - \varepsilon^{Tt}\right), \tag{6}$$

where σ is the uniaxial stress, ε is the uniaxial strain, and E is the elastic modulus.

Next, the strength of materials solution is examined for two separate bars constructed from the same material, with properties as shown in Figure 8. Both bars are initially set at a reference state of zero load and zero temperature. The loading histories for bars one and two are shown in Figure 9. The axial strain in bar number one can be found from strength of materials theory to be

$$\varepsilon_{t_1}^{1} = \alpha\Delta T + \frac{\sigma}{E} = 10 \times 10^{-6} \times 100 + \frac{10000}{10^{7}} = .002. \tag{7}$$

Similarly, the axial strain in bar number two is determined to be

$$\varepsilon_{t_2}^{2} = \alpha\Delta T + \frac{\sigma}{E} = 20 \times 10^{-6} \times 200 + \frac{10000}{5 \times 10^{6}} = .006. \tag{8}$$

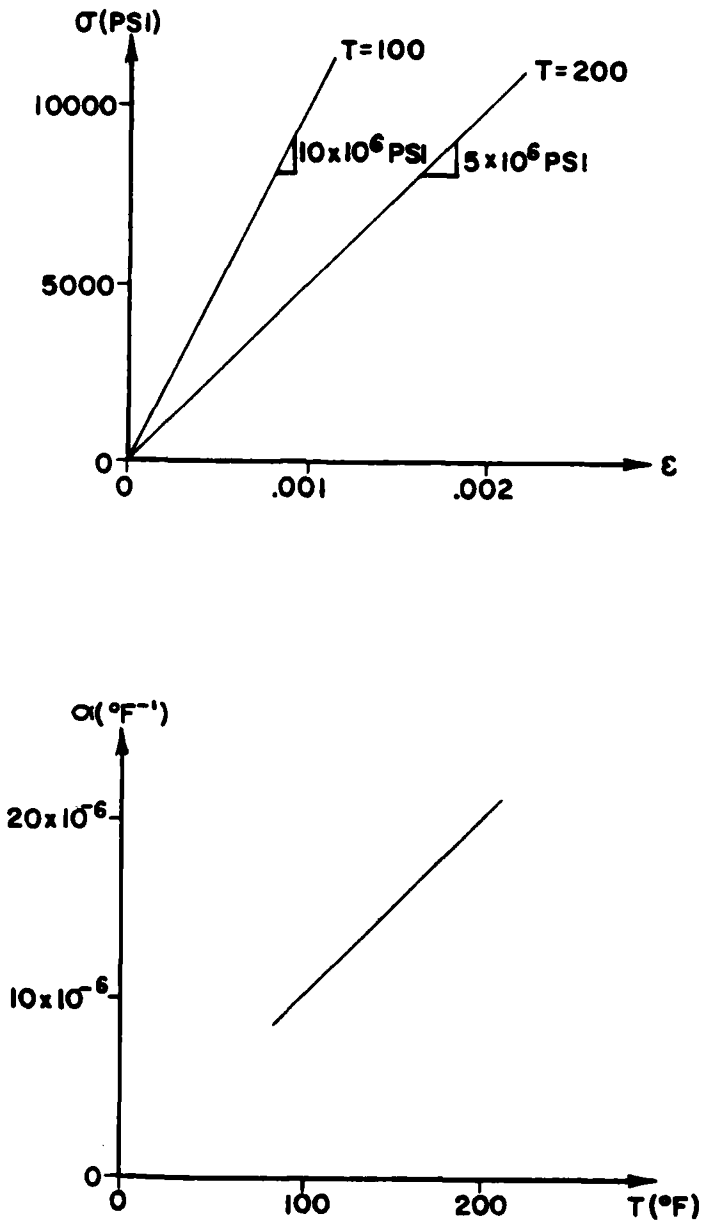

Figure 8. Material Data for Nonisothermal Elastic Uniaxial Bar

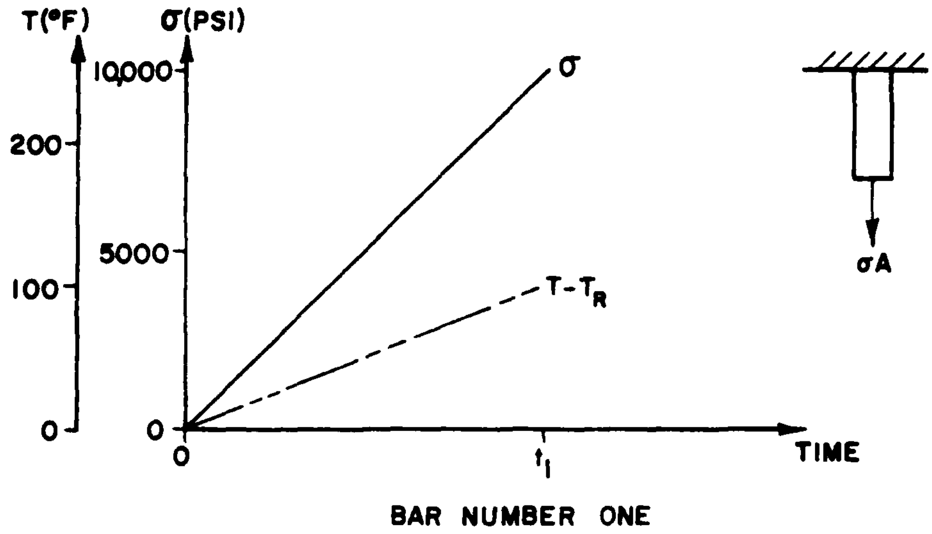

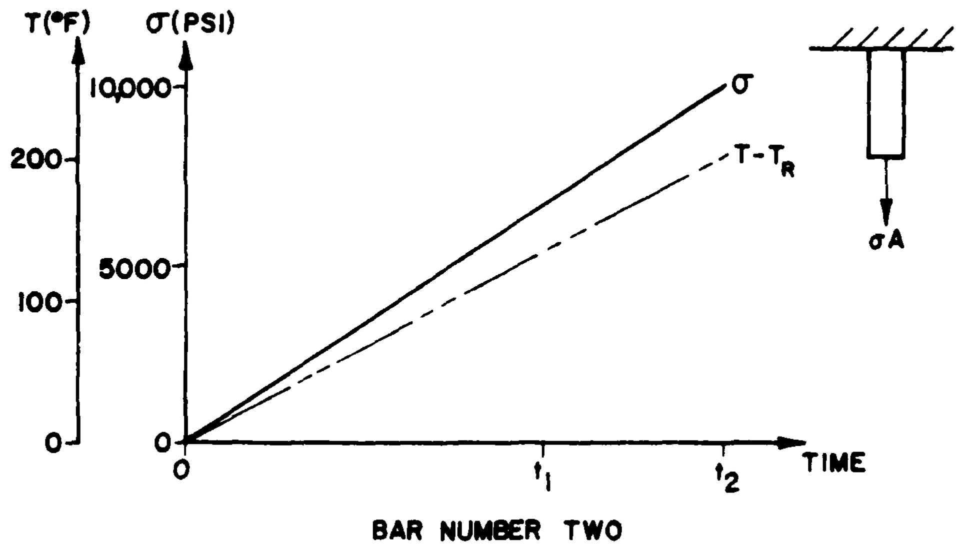

Figure 9. Load Histories for Nonisothermal Elastic Uniaxial Bar Test Cases One and Two

Next, bar number one is subjected to the additional loading history shown in Figure 10. Since for elastic action the loading history must be path independent, it is seen that the axial strain in bar number one must now be identical to that in bar number two. Thus, the strain increment predicted in bar number one for the time increment from t_1 to t_2 must be the difference in the total strains determined in equations (7) and (8), or .004 in/in. Hence, in order to be correct, equation (7) must predict this result.

Suppose one assumes that the thermal strain increment is given by

$$d\varepsilon^T = \alpha^{t+\Delta t} \; (T_{t_2} - T_{t_1}) = 20 \times 10^{-6} \times 100 = .002. \qquad (9)$$

Then, noting that the stress increment is zero, equation (6) gives

$$0 = 5000000 \; (d\varepsilon - .002) + (-5000000) \; (.002 - .001) \rightarrow$$

$$d\varepsilon = .002 + \frac{5000000}{5000000} \; (.002 - .001) = .003. \qquad (10)$$

The above prediction is obviously in error. This error can be traced to the thermal strain increment determined in equation (9). Suppose on recalculates the thermal strain increment assuming

$$d\varepsilon^T = \alpha^{t+\Delta t} \; (T_{t_2} - T_R) - \alpha^t \; (T_{t_1} - T_R)$$

$$= 20 \times 10^{-6} \; (200-0) - 10 \times 10^{-6} \; (100-0) = .003. \qquad (11)$$

For the above predicted thermal strain increment equation (6) gives

$$0 = 5000000 \; (d\varepsilon - .003) + (-5000000) \; (.002 - .001) \rightarrow$$

$$d\varepsilon = .003 + \frac{5000000}{5000000} \; (.002 - .001) = .004, \qquad (12)$$

which is the correct increment. To better see how the error is incurred

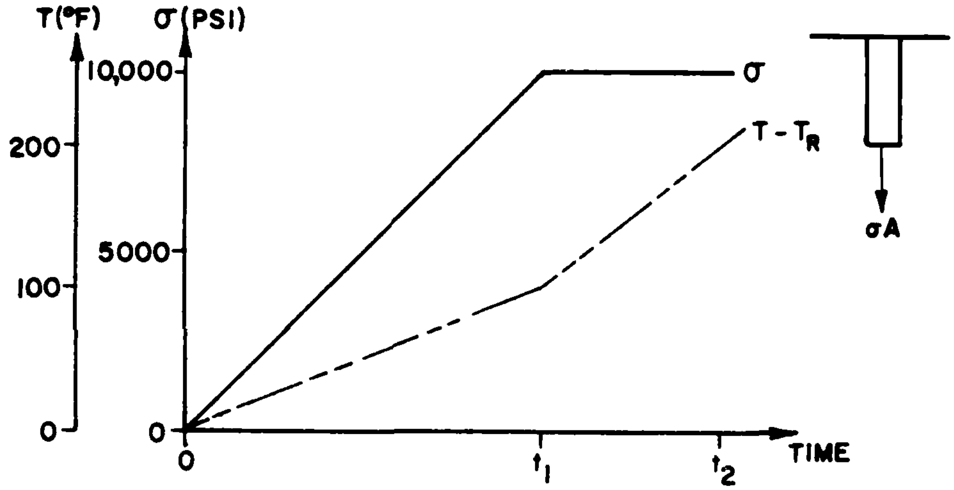

Figure 10. Load History for Nonisothermal Elastic Uniaxial Bar Test Case Number Three

by using the former definition, consider the latter definiti.., given by equation (11)

$$d\varepsilon^T = \alpha^{t+\Delta t} (T_{t_2} - T_R) - \alpha^t (T_{t_1} - T_R)$$

$$= \alpha^{t+\Delta t} (T_{t_2} - T_{t_1}) + (\alpha^{t+\Delta t} - \alpha^t) (T_{t_1} - T_R). \tag{13}$$

The first term in equation (13) is the thermal strain increment predicted by equation (9), and the second term therefore represents the error incurred by using equation (9). Mathematically, equation (13) may be interpreted as representing a chain rule differentiation. Physically, the last term can be better understood by considering an example. Consider a uniaxial bar subjected to an initial thermal and mechanical load. Now suppose that some process can be performed on the bar such that the coefficient of thermal expression can be altered without changing the temperature. Then the bar will undergo an additional expansion given by the second term in equation (13). It can be seen that the error incurred by neglecting his term will depend on how strongly alpha depends on temperature. It should not be assumed that because this term is small for a particular load step that it may be neglected. Rather, the entire load history should be considered. If there is a significant variation in the coefficient of thermal expansion for the range of temperatures expected, this term should not be neglected.

To illustrate the error which may be incurred by utilizing equation (10) to define the thermal strain increment, the code is now compared to experimental data. An aluminum (6061-T6) axial bar with material properties as shown in Figure 11 is subjected to the load history shown

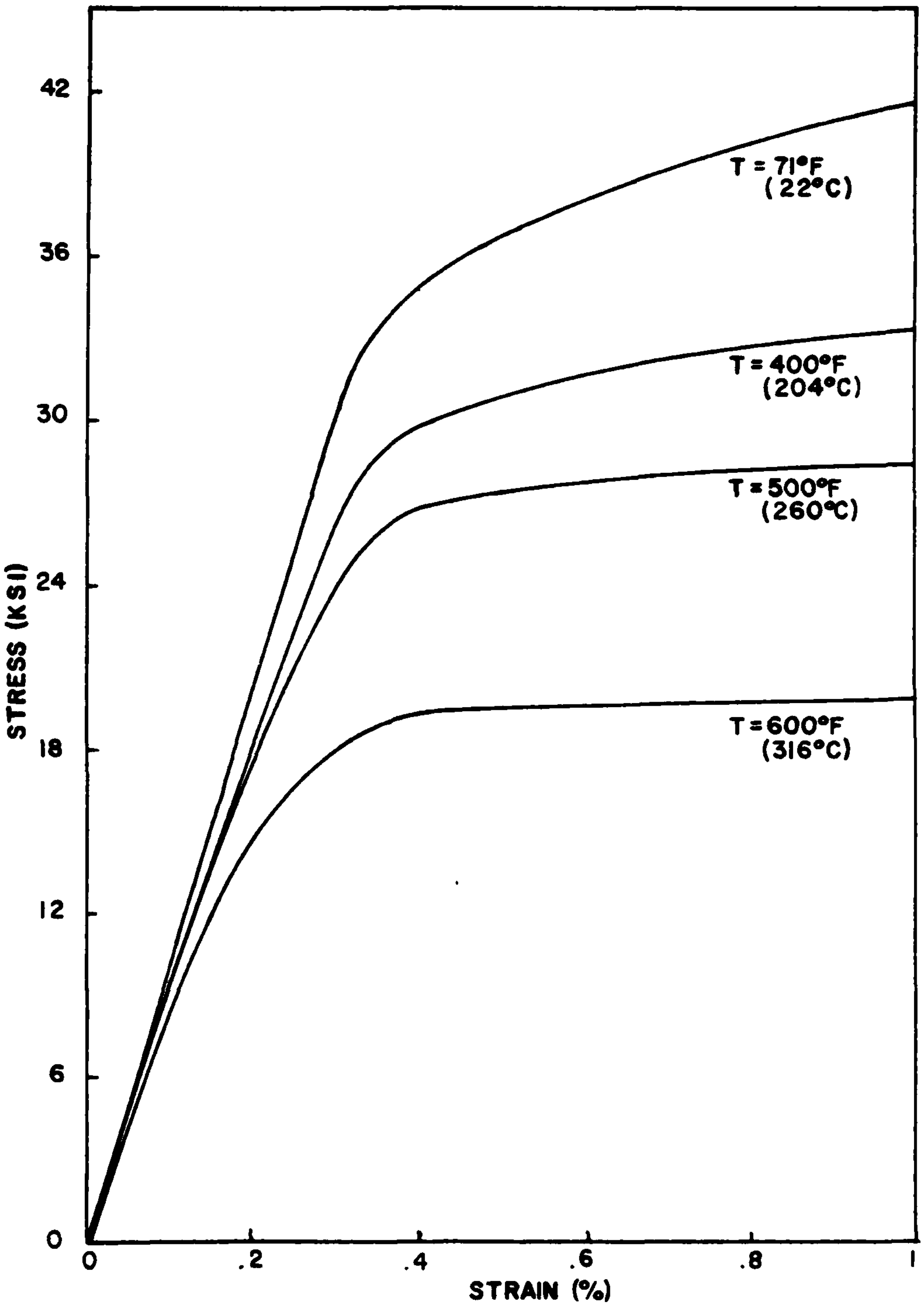

Figure 11. Material Data for Al 6061-T6 Experimental Test Samples

in Figure 12. Due to the relatively short time period, creep strain is assumed to be negligible. Analytical axial strain calculations are compared to experiment in Figure 12. Experimental results as well as the theoretical result denoted CREEPARHS are due to Stone.[10] Three solutions were performed in AGGIE I using a single plane stress isoparametric element and twenty-six load steps. In the first analysis it is assumed that material properties are not temperature dependent and room temperature data are used. In the second solution, properties are assumed to vary with temperature, and the definition of the thermal strain increment given by equation (9) is used. Finally, the third analysis employs temperature dependent material properties as well as the definition of the thermal strain increment given in equation (11). It is found that all theoretical results except the last are in error by approximately ten percent or more. Thus, the importance of temperature dependent material properties as well as a correct definition of the thermal strain increment are illustrated by this example problem.

V. Quasi-Isothermal Elastic-Plastic Annular Disk Subjected to Radial Temperature Variation

In this example problem the annular disk shown in Figure 13 is subjected to a heat input producing a static temperature distribution given by

$$T = T_a - (T_b - T_a) \log (r/a) / \log (b/a), \qquad (14)$$

where T_b is the temperature at the outer surface and T_a is the temperature at the inner surface. It is found that under this loading condition the material yields, thus requiring an elastic-plastic constitutive theory. For this anlysis the uniaxial stress-

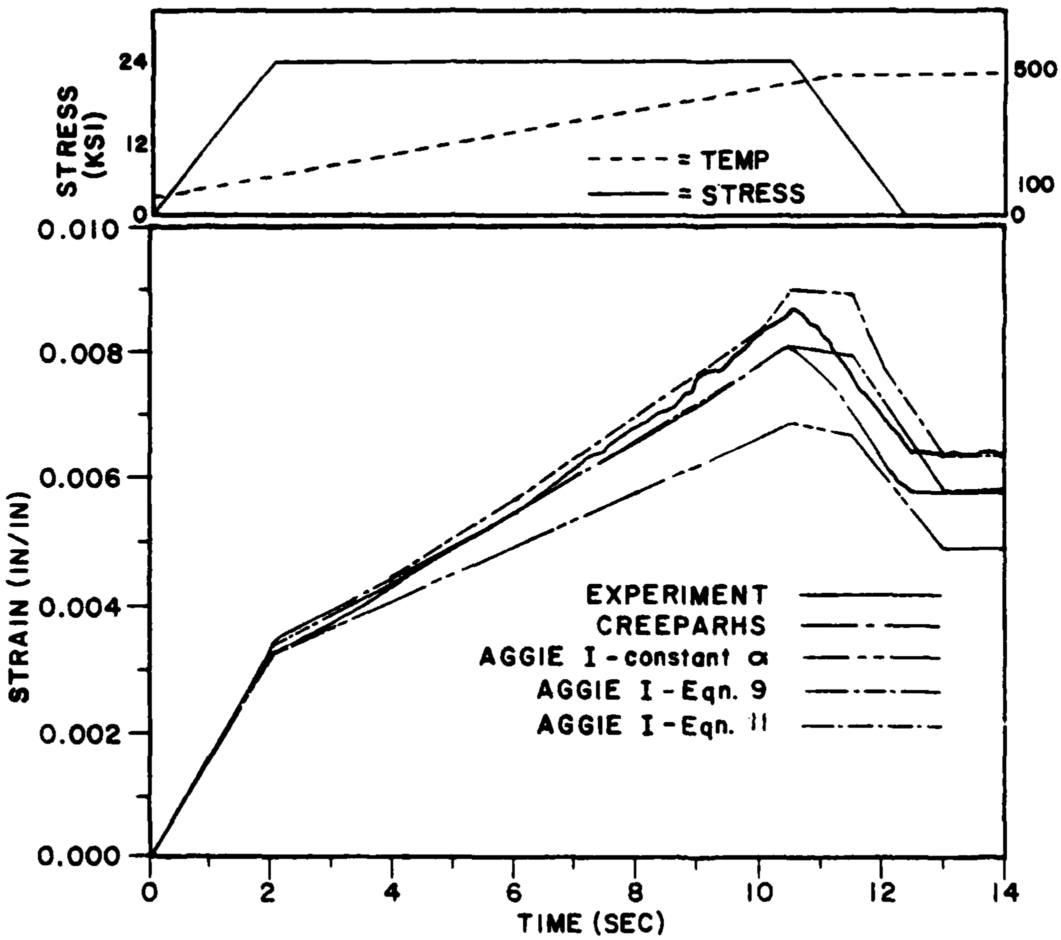

Figure 12. Comparison of Analysis to Experiment for Example Four

strain data and finite element mesh shown in Figure 13 were used. A theoretical solution to this problem has been obtained by Dastidar and Ghosh,[11] and duplicated by Levy.[12] We have solved this problem using both the quasi-isothermal elastic-plastic and the nonisothermal elastic-plastic models in AGGIE I. In the second model it was assumed that the material exhibited identical uniaxial stress-strain behavior at various temperatures, thus reproducing the results obtained in the quasi-isothermal. The purpose of this example problem is twofold. First, it is shown in Figure 14 that the quasi-isothermal elastic-plastic theory within AGGIE I produces results for radial stress (σ_r) and hoop stress (σ_θ) which are identical to those obtained by others.[11,12] Second, it is noted here that utilizing the quasi-thermal constitutive model in AGGIE I gave a computational time saving of approximately 4.5% when compared to the nonisothermal theory. Therefore, it is concluded that the use of simplified theories when material properties of the medium are essentially temperature independent can be efficient nd should be included as separate models within the computer codes.

VI. Nonisothermal Elastic-Plastic Axial Bar

This test case demonstrates the capability of the code to predict the response of media near their ultimate strength. As a part of this ability it is necessary to properly predict the structural response in the transition range from elastic to elastic-plastic behavior. A method for predicting isothermal behavior in the transition range has been previously proposed by Krieg and Duffey.[13] Although their approach may not be used during nonisothermal transitions, it can be modified to obtain correct results. This method will be presented here along

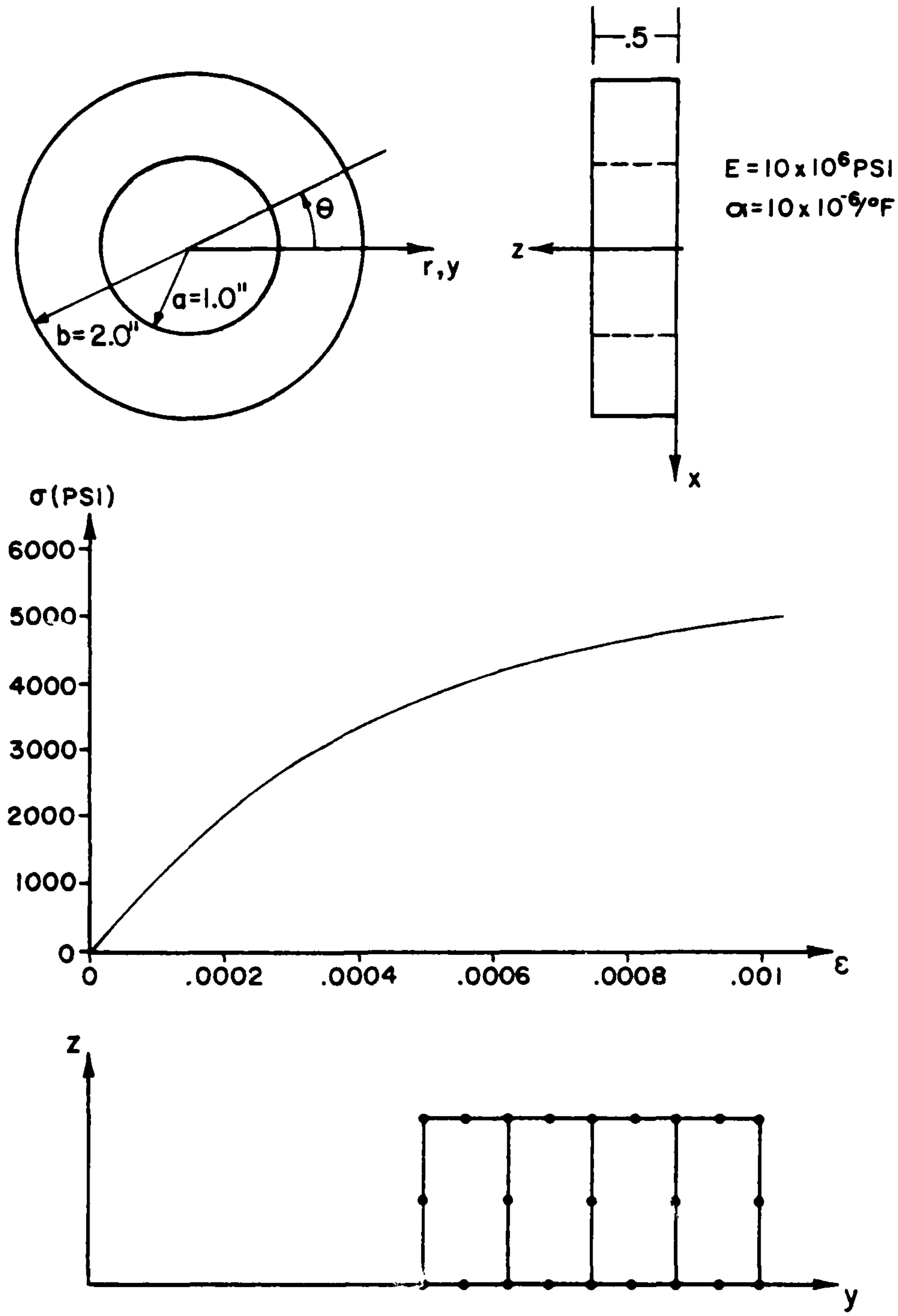

Figure 13. Input Data for Example Five

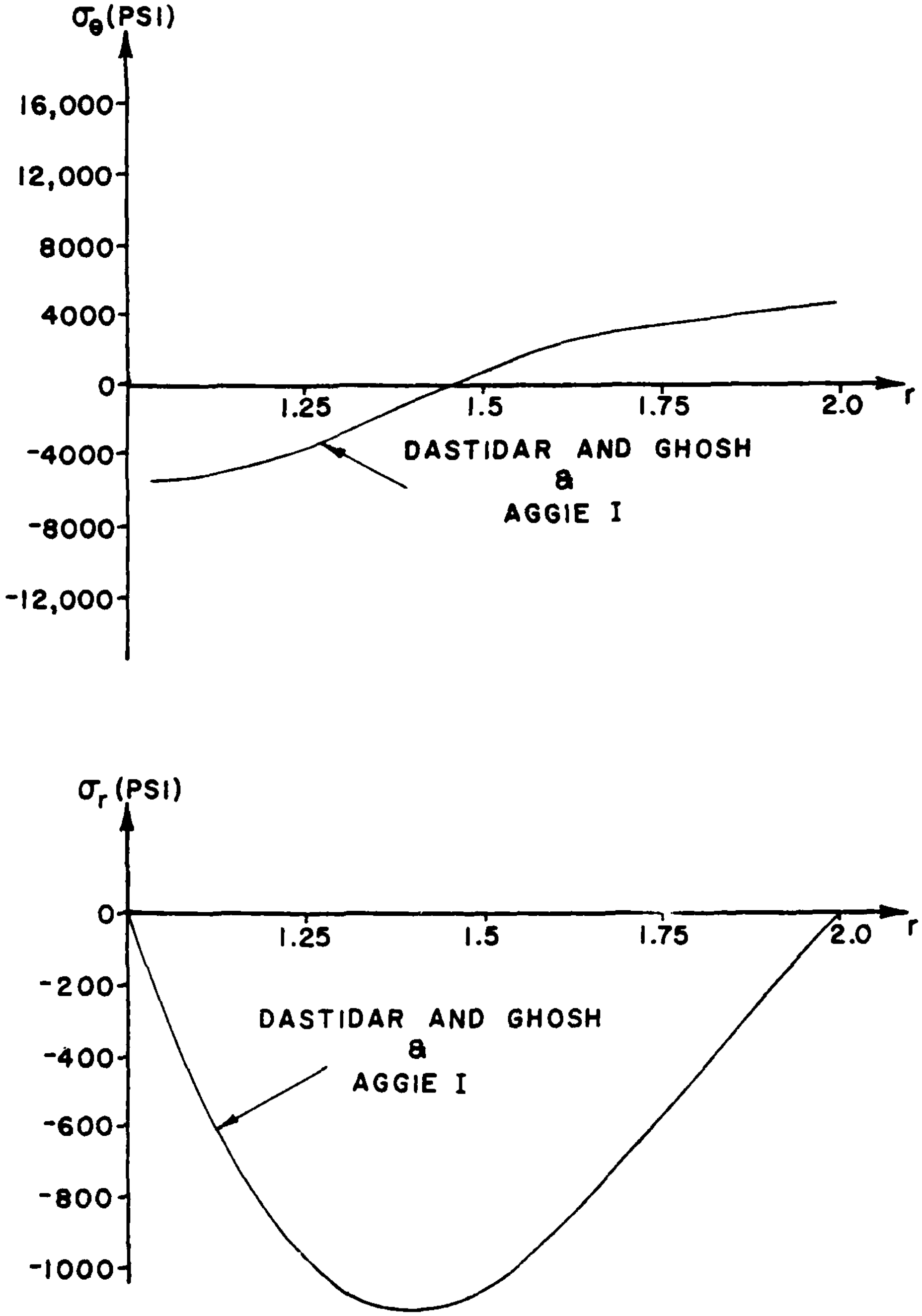

Figure 14. Comparison of Analyses for Example Five

with a verifying example.

First recall that an assumed stress increment tensor ($d\hat{S}_{ij}$) is obtained using the predicted strain increment tensor dE_{ij} and assuming elastic behavior, i.e.,

$$d\hat{S}_{ij} = D_{ijmn}^{t+\Delta t} (dE_{mn} - dE_{mn}^{C} - dE_{mn}^{T}) + dD_{ijmn} (E_{mn}^{t} - E_{mn}^{Ct} - E_{mn}^{Tt}) \tag{15}$$

where the quantities above are as previously defined. This supposed stress increment tensor is then added to the stress state at the start of the step and the sum is used to check for plastic flow via the yield condition.[1,2] If no yielding occurs the predicted stress increment is correct. However, if the yield condition is satisfied, one must first determine that portion of the stress and strain to the initial yield surface.

To obtain the stress increment tensor necessary to cause yield, recall that the yield function is utilized, i.e.,

$$(S_{ij}' + \zeta d\hat{S}_{ij}' - \alpha_{ij}') (S_{ij}' + \zeta d\hat{S}_{ij}' - \alpha_{ij}') = \frac{2}{3} \sigma_{y}^{t+\Delta t^{2}} , \tag{16}$$

where α_{ij} is the yield surface translation tensor, $\sigma_{y}^{t+\Delta t}$ denotes that the yield surface size is temperature dependent, primes indicate deviatoric components, and $\zeta d\hat{S}_{ij}'$ is the stress increment tensor necessary to cause yielding. In this respect the method proposed by Krieg and Duffey is correct. Recall that one determines ζ by using

$$\zeta = \frac{-B + \sqrt{B^2 - 4AC}}{2A} , \tag{17}$$

where

$$A = d\hat{S}'_{ij}\ d\hat{S}'_{ij} \quad ,$$

$$B = 2\ (S'_{ij} - \alpha'_{ij})\ d\hat{S}'_{ij}, \text{ and} \tag{18}$$

$$C = (S'_{ij} - \alpha'_{ij})\ (S'_{ij} - \alpha'_{ij}) - \frac{2}{3}\ {\sigma_y^{t+\Delta t}}^2 \quad .$$

In order to find the strain increment tensor necessary to cause yielding, the isothermal theory must be modified. To do this, first note that since the material behaves elastically up to yield, the following relation must be satisfied:

$$(S^t_{ij} + \zeta d\hat{S}_{ij}) = D^{t+\Delta t}_{ijmn}\ (E^{et}_{mn} + \mu d\hat{E}^e_{mn}) \ , \tag{19}$$

where μ is a scalar which when multiplied by the predicted elastic strain increment $d\hat{E}^e_{mn}$, will cause yielding, and the superscript e denotes elastic strain components. Solving equation (19) for μ and setting the free indeces i and j equal to unity yields.

$$\mu = \frac{S^t_{11} + \zeta d\hat{S}_{11} - D^{t+\Delta t}_{11mn}\ E^{et}_{mn}}{D^{t+\Delta t}_{11kl}\ d\hat{E}^e_{kl}} \tag{20}$$

Since

$$S^t_{11} = D^t_{11mn}\ E^{et}_{mn} \quad , \tag{21}$$

equations (20) and (21) may be combined to obtain

$$\mu = \frac{\zeta d\hat{S}_{11} - dD_{11mn}\ E^{et}_{mn}}{D^{t+\Delta t}_{11kl}\ d\hat{E}^e_{kl}} \tag{22}$$

Thus, after obtaining ζ from equation (17) one can find μ in equation (22) and the resulting strain increment tensor necessary to cause yielding from

$$\overset{y}{dE}{}^e_{mn} = \mu d\hat{E}^e_{mn} \quad . \tag{23}$$

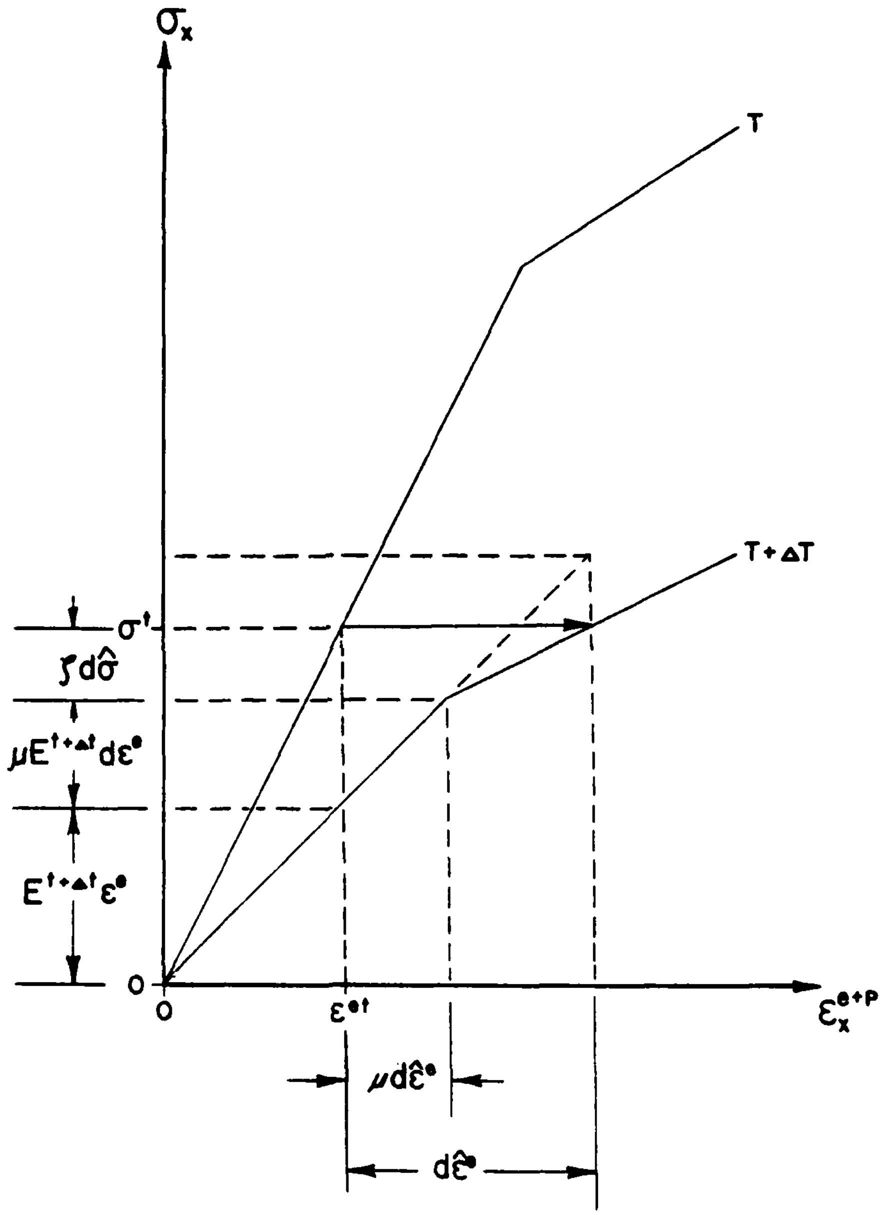

Figure 15. Uniaxial Case for Transition Stress Increment Determination

The method in equation (23) may be better understood by considering a uniaxial case, as shown in Figure 15. For a one dimensional stress state equation (20) reduces to

$$\mu = \frac{\sigma^{t} + \zeta d\hat{\sigma} - E^{t+\Delta t}\ \varepsilon^{et}}{E^{t+\Delta t}\ d\hat{\varepsilon}^{e}} \tag{24}$$

where σ is the uniaxial stress, ε is the uniaxial strain, and E is the elastic modulus. For convenience the thermal and creep strains are removed from the graph in Figure 15 so that on the ordinate it is found that

$$\sigma^{t} = E^{t+\Delta t}\ \varepsilon^{et} + \mu E^{t+\Delta t}\ d\varepsilon^{e} + \zeta d\hat{\sigma} \quad . \tag{25}$$

Solving the above equation for μ gives equation (24) so that the theory is verified for the uniaxial case.

In order to complete the constitutive law for the transition step from elastic to plastic action it is next necessary to determine the portion of the strain increment occurring after yield. This amount is given by

$$dE_{ij}^{ep} = (1-\mu)\ d\hat{E}_{ij} \quad . \tag{26}$$

Now again considering Figure 15, it is seen that since the state of stress and strain have been advanced to the stress-strain curve for the temperature at the end of the step, one need only calculate the isothermal portion of the stress increment caused by dE_{ij}^{ep}. In other words, in the transition step the term dP_{ij} may be dropped from equation (1). Due to the determination of the stress increment necessary to cause yielding this final step will yield correct results.

It is interesting to note that equation (1) may be used without modification if a different formulation for ζ is used. In fact, $d\hat{S}_{ij}$ may be used as the stress increment necessary to cause yielding if equation (1) is used to predict the stress increment after yield. This method has not been used here for two reasons. First, it is obviously computationally efficient to circumvent the calculation of dP_{ij} due to its complexity. Second, and more importantly, the uniaxial thermal stress rate ($d\sigma/dt$) necessary to calculate dP_{ij} cannot be determined below the yield point because the computer code AGGIE I does not save this information. For other reasons which are apparent from examination of references 1 and 2, the code carries only data relating uniaxial stress to plastic strain.

The above method may now be applied to an example experimental problem. In this example an axial bar with isothermal material properties shown in Figure 16 is subjected to the load history shown in the same figure. Attempts at verification of this problem have failed due to the fact that the relatively long heat-up time required with the equipment at this institution induces significant creep. Additional equipment is on order and it is hoped that experimental verification will be forthcoming in the near future. This example is included not as a verification of the theory, but rather as a corroboration of the computational efficiency of the model.

One will recall that in our previous papers[1,2] we proposed that to obtain the effective modulus tensor C_{ijmn} for a load step one should use the elastic constitutive tensor D_{ijmn} at the end of the load step. This was shown to be mathematically correct and is computationally supported by this example. In the example, an axial bar is loaded

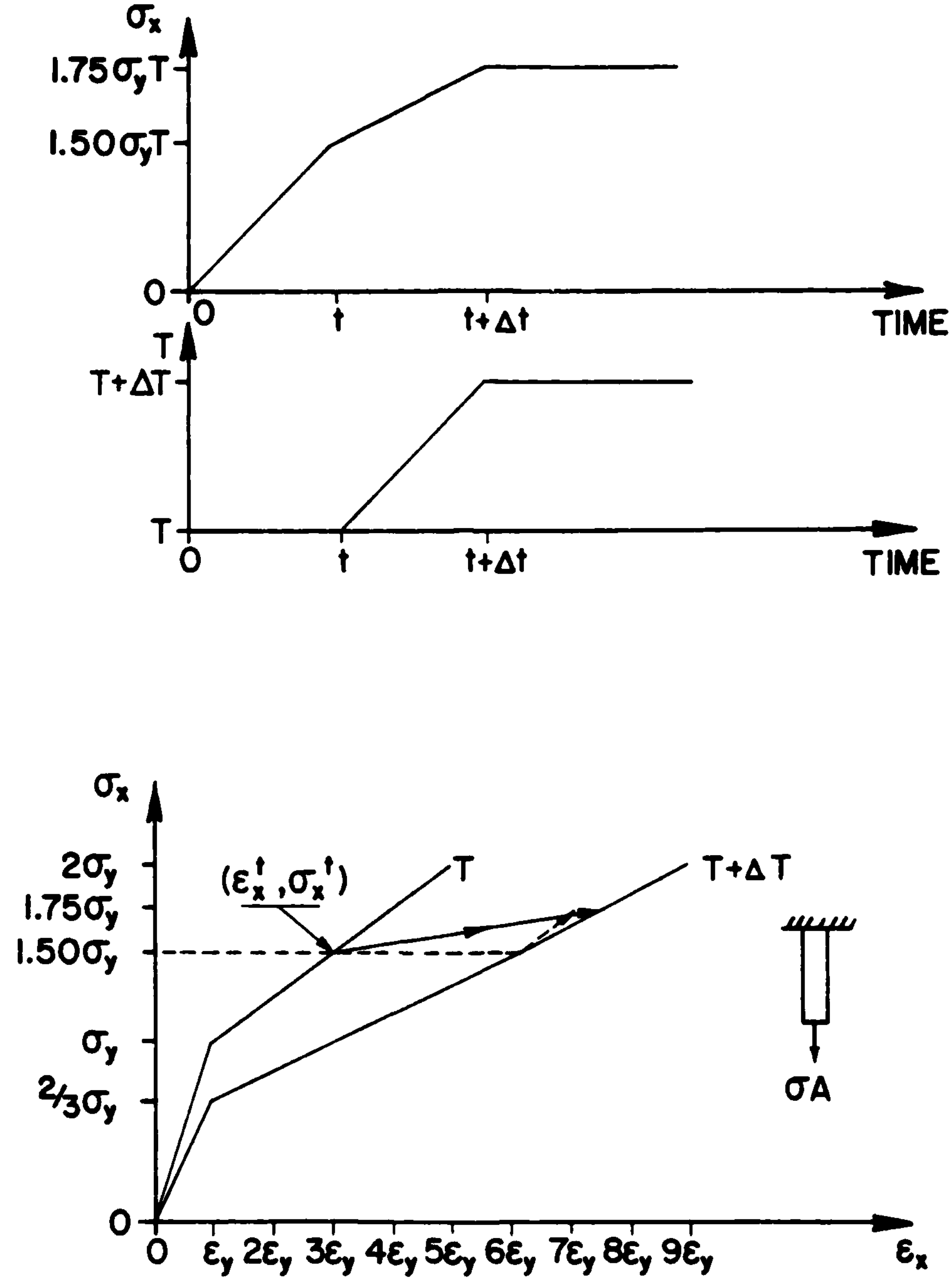

Figure 16. Results for Example Six

isothermally to some plastic state and is then simultaneously subjected to a mechanical load and spacially constant slow heat input. According to the classical incremental theory of plasticity it is required that the state of stress and strain move to a point on the uniaxial stress-strain diagram for the temperature at the end of the step. This requirement must be satisfied in order to remain consistent with the yield surface during plastic loading. Using the elastic modulus proposed by us the theory will predict this result exactly. If one utilizes the elastic modulus at the start of the load step the state of stress and strain will converge incorrectly to a point denoted by the head of the dashed line in Figure 16. This point corresponds to a horizontal translation from $(\varepsilon_x^t, \sigma_x^t)$ to the stress-strain curve at the temperature at the end of the step, followed by a translation parallel to the stress-strain curve at time t. Thus, utilizing the elastic modulus at the start of a load step does not satisfy the consistency condition. Further, if one employs equilibrium iteration and correctly updates the elastic modulus during the iteration procedure, the solution will converge to the correct solution, but in exactly twice the computation time encountered in our theory. Therefore, it is suggested that using the elastic constitutive tensor at the end of the step is not only consistent but also computationally efficient.

VII. Nonisothermal Elastic-Plastic Axial Bar with Significant Creep

This test case demonstrates the capability of the code to predict the response of media near their ultimate strength. As was pointed out in references 1 and 2, a part of this ability rests upon properly predicting the structural response in the transition range from elastic to elastic-plastic behavior. To demonstrate this capability, an aluminum (6061-T6) uniaxial bar with isothermal material properties shown in Figure 11 is subjected to the load history shown in Figure 17, such that ultimate failure of the specimen occurs. Experimental and CREEPARHS results for axial strain are due to Stone.[10] Two analyses were performed using AGGIE I. In the first, creep is assumed to be negligible. In the second, linear interpolation of isothermal creep data at a load of 20 KSI is used. It is seen from results plotted in Figure 17 that the theory produces accurate results even near the ultimate strength of the material.

VIII. Nonisothermal Elastic-Plastic Thick Walled Cylinder

In this problem an axisymmetric cylinder with material properties and geometry shown in Figure 18 is subjected to the thermomechanical load history shown in the same figure. Residual radial stresses and displacements at time t = 10 are shown in Figure 19, indicating that results obtained in AGGIE I are comparable to those obtained in ADINA.[3] This example was chosen because the author has been unsuccessful in obtaining documented experimental results of bodies subjected to thermomechanical loadings producing spacially variable multiaxial stress states. It is to be noted that the model in ADINA does not account for combined hardening during cyclic loading, and thus represents a special case of the model proposed herein.

IX. History Dependent Uniaxial Thermomechanical Loadings

Although no experimental results are available for this example, it serves to illustrate the capability of the theory to model history dependent phenomena. In the analysis, four identical uniaxial bars with isothermal material data as shown in Figure 20 and initially at

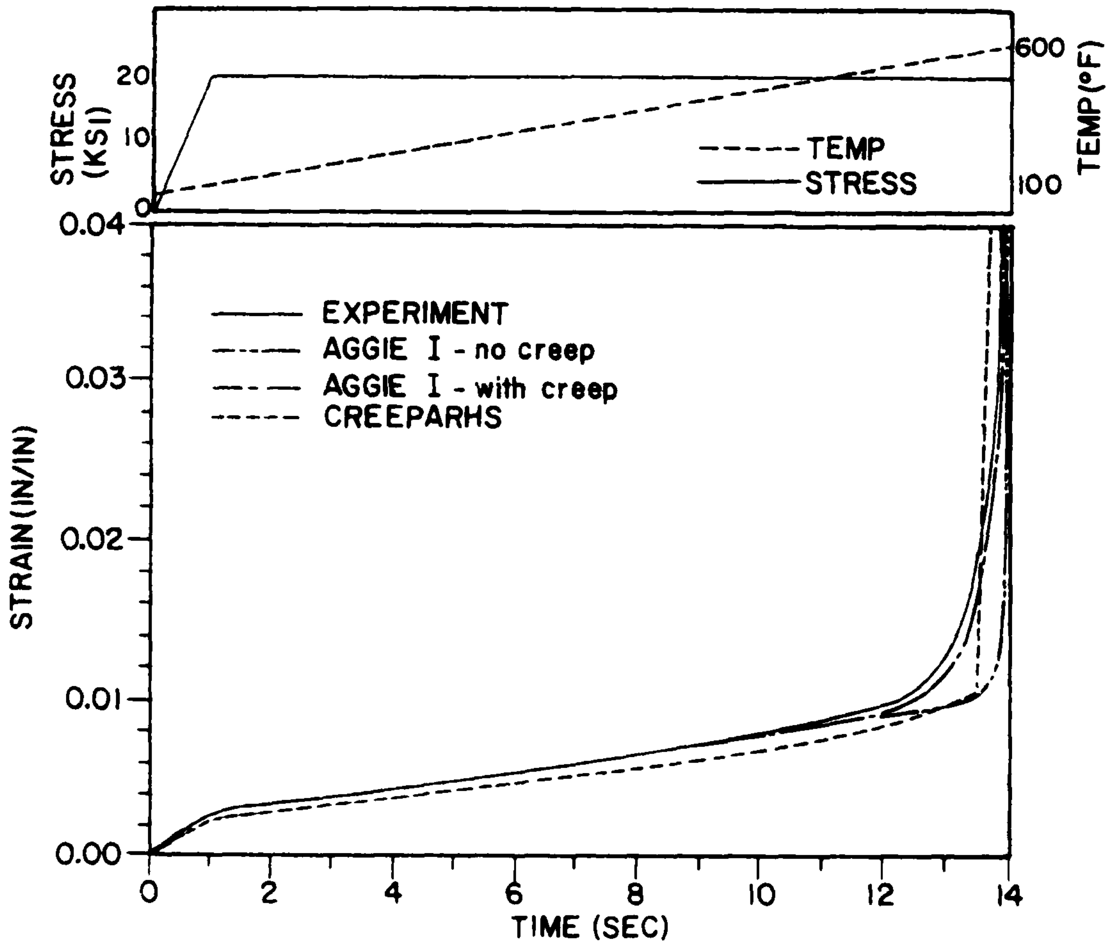

Figure 17. Comparison of Analysis to Experiment for Example Seven

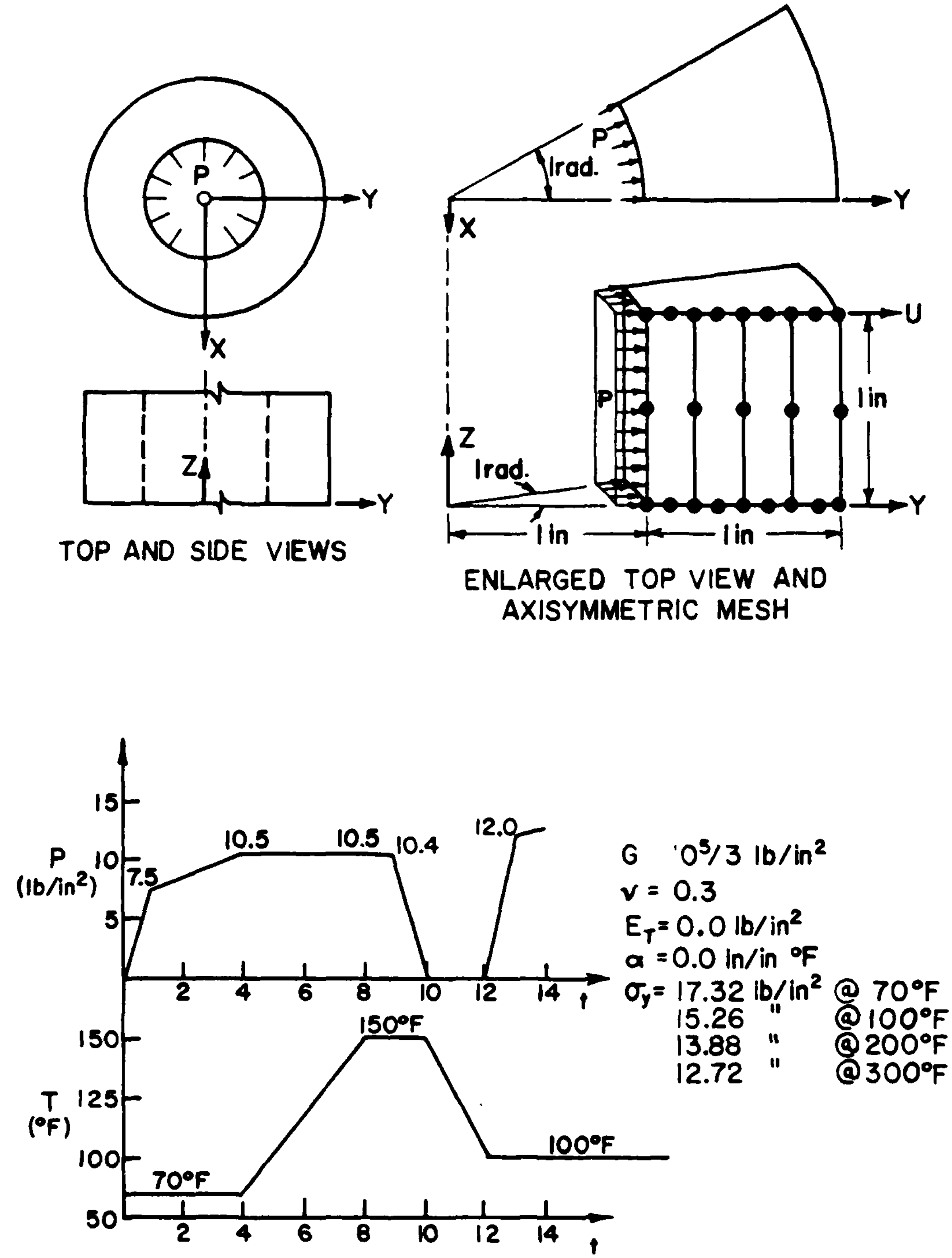

Figure 18. Input Data and Thermomechanical Loading for Example Eight

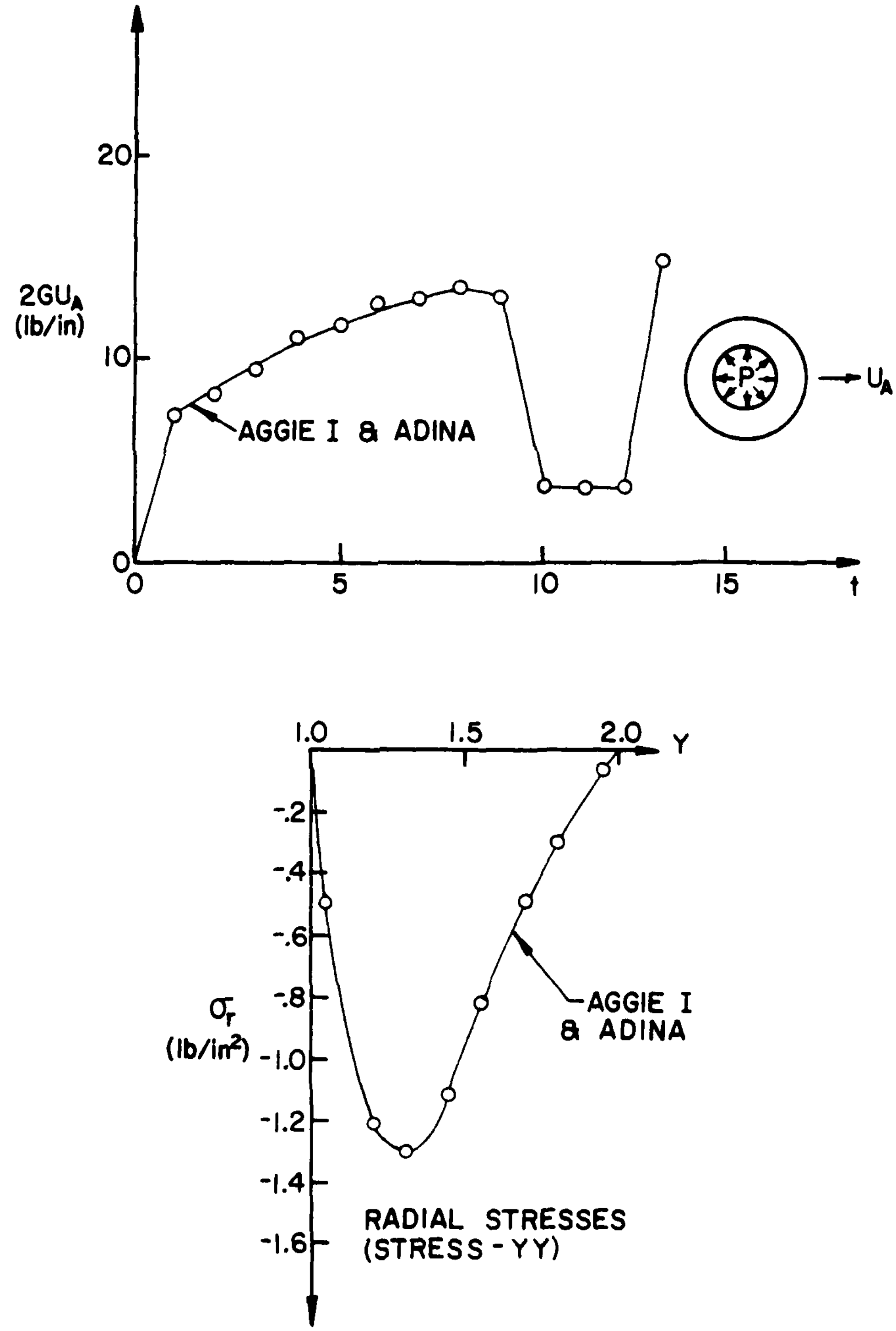

Figure 19. Comparison of Analyses for Example Eight

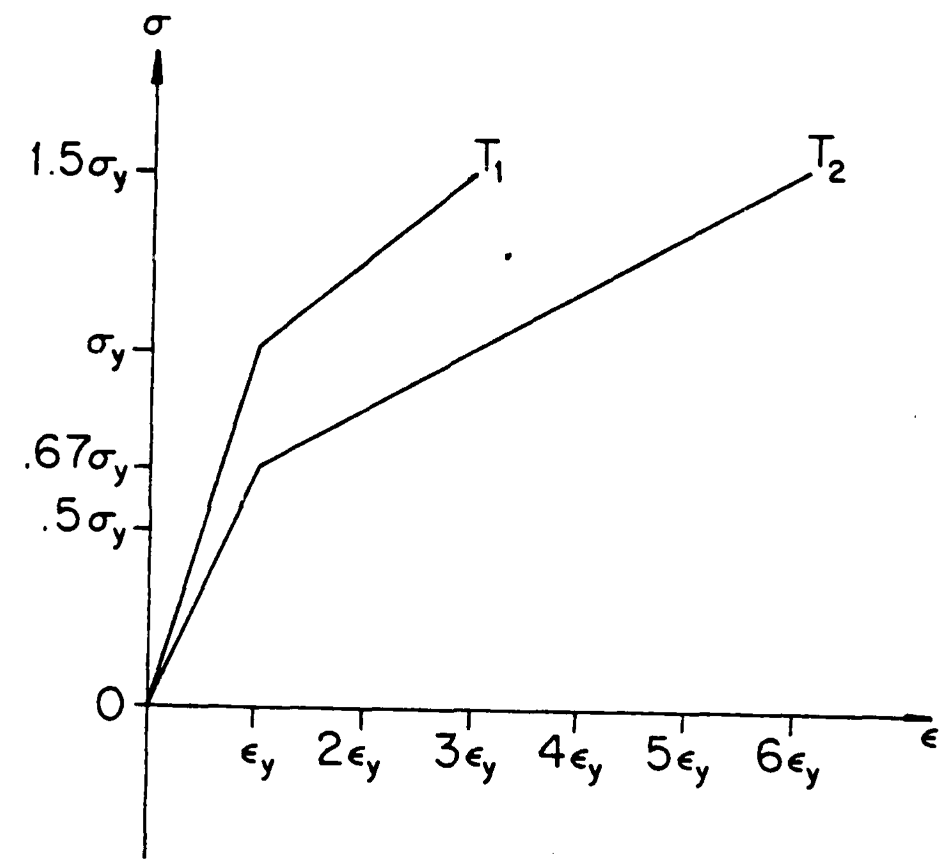

Figure 20. Material Data for Example Nine

zero load and temperature are subjected to the thermomechanical loadings shown in Figures 21 and 22. It is noted that the peak thermomechanical load in each case is identical. Results of the theory are shown in Figure 23, wherein it is seen that the model does in fact predict significantly different residual strains.

X. Nonisothermal Elastic-Plastic Axial Bar Subjected to Cyclic Load Histories

One of the primary purposes of this research has been to obtain a theory which can effectively model the response of elastic-plastic media to cyclic mechanical and thermal loading. Although the literature contains abundant verification tools for isothermal cyclic loading histories, the author has been unable to obtain experimental data to verify the nonisothermal problem. Therefore, certain experiments have been undertaken to perform certain nonisothermal tests using axial bars on the MTS system. Although results of these experiments are incomplete at this time, analytical results of a cyclic test are presented herein. Although the theory is capable of modelling creep response, this study is meant to verify the time independent behavior of the material. Therefore, the uniaxial test case shown in Figure 24 has been chosen. Note that the specimen is heated at zero load after prestrain so that no creep occurs. This problem thus tests the expansion and translation of the yield surface in stress space caused by a temperature change. In order to verify the applicability of the theory it is necessary to perform three material data tests. Isothermal stress-strain curves are generated at room temperature and 200°F. In addition, an isothermal cyclic load test is performed to determine the ratio of isotropic to kinematic hardening (β) used in the model. Theoretical results are presented in

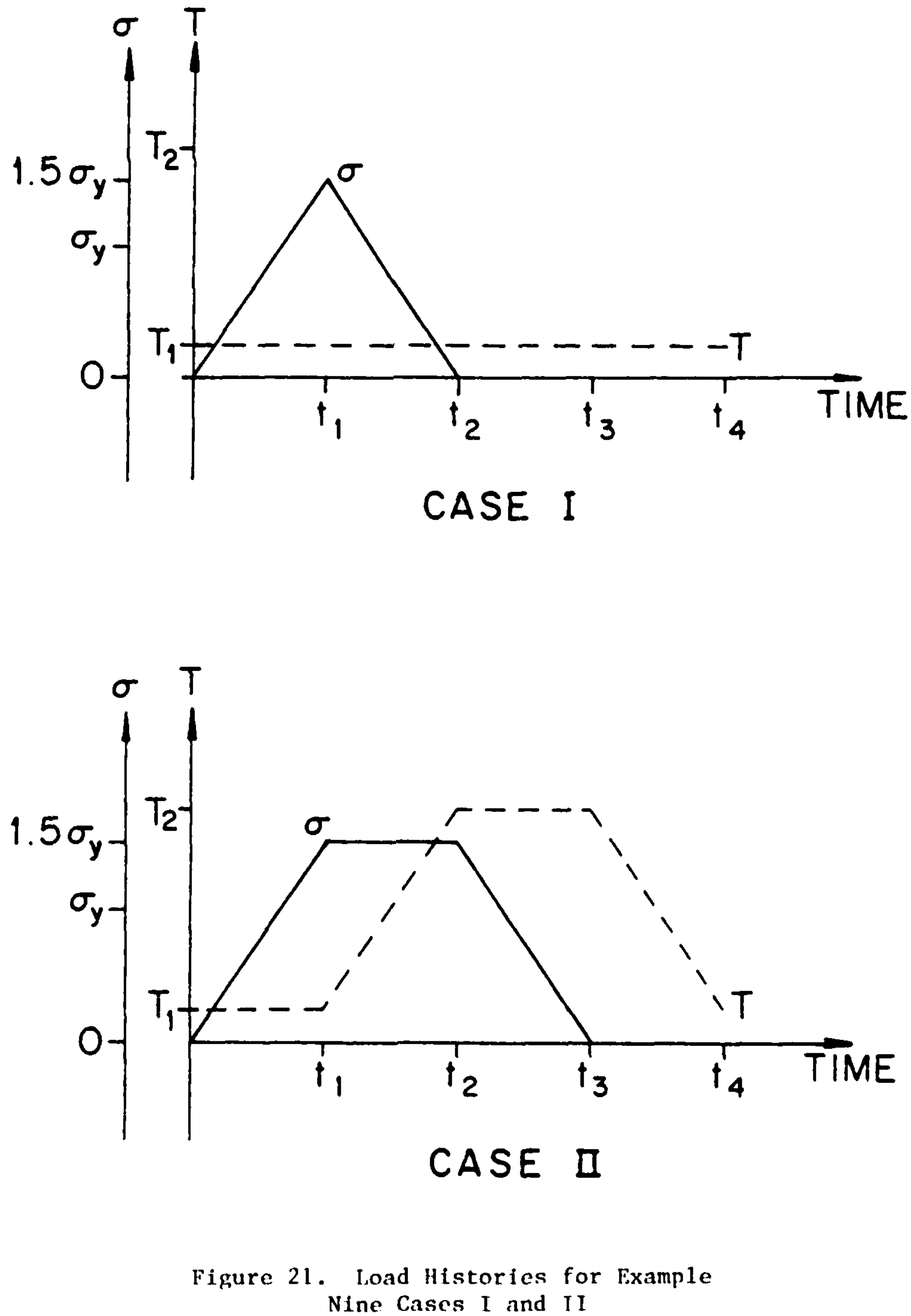

Figure 21. Load Histories for Example Nine Cases I and II

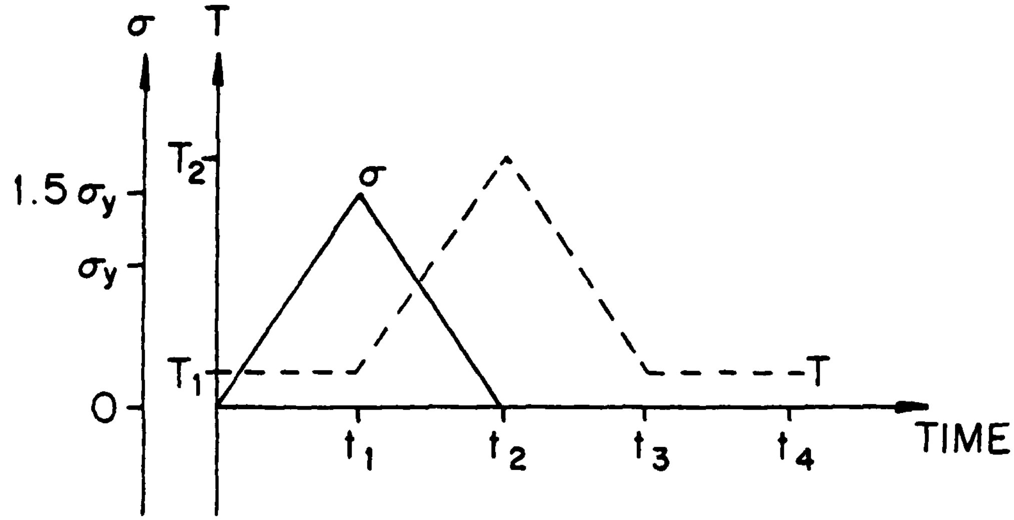

CASE III

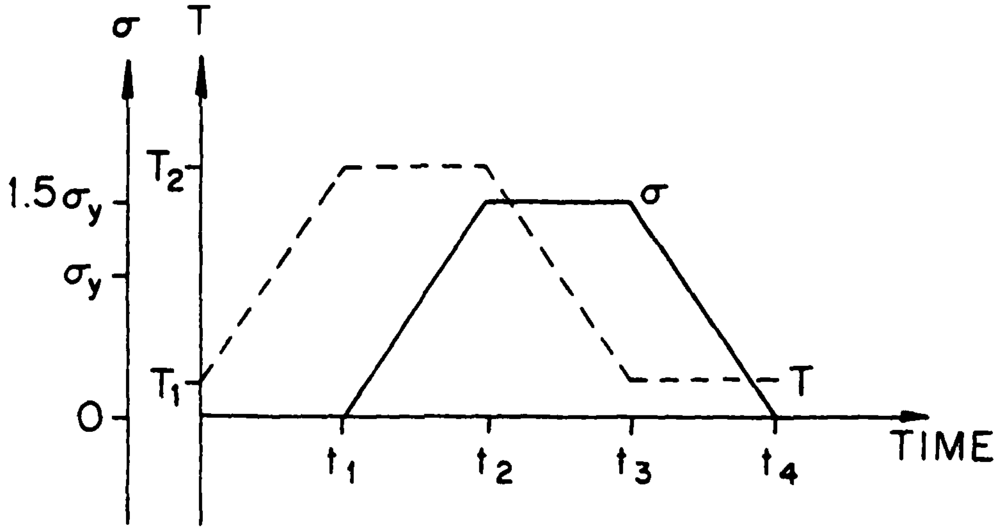

CASE IV

Figure 22. Load Histories for Example
Nine Cases III and IV

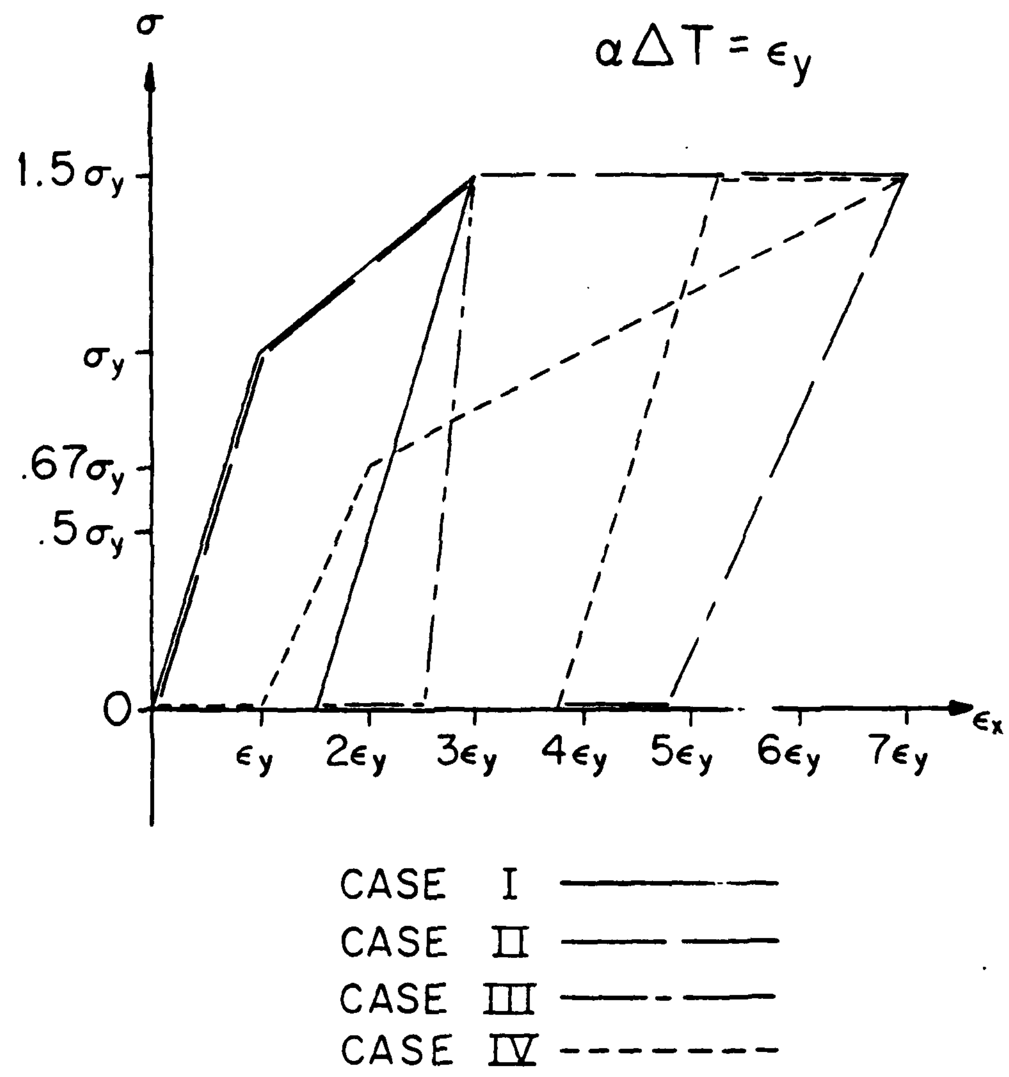

Figure 23. Results for Example Nine

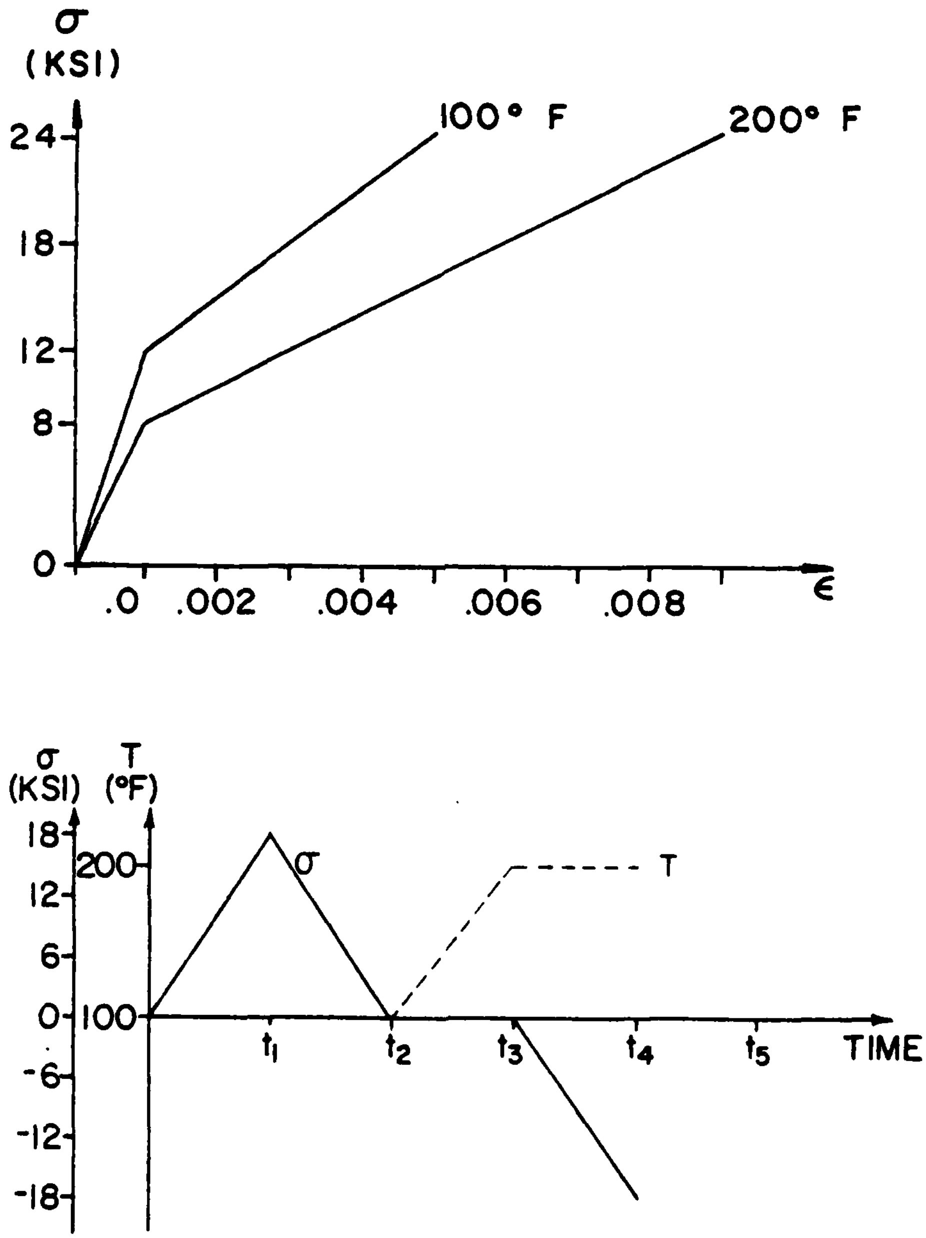

Figure 24. Material Data and Loading for Example Ten

Figure 25 where it should be noted that the times t_i correspond to those shown in the load history curve in Figure 24. It is seen that the combined hardening model (t_4^c) with β = .5 produces results which differ significantly from both kinematic (t_4^k) and isotropic (t_4^I) nonisothermal hardening theory as well as isothermal isotropic hardening theory at time t_4, indicated by the dashed line in Figure 25.

In order to better understand the genesis of the yield surface for the various workhardening rules, the yield surface is diagrammed for the various workhardening rules in Figures 26 through 28. Note again that the times t_i in these figures correspond to those shown in Figure 24. The arrows shown along the α_1 axis in each diagram represent the path of the stress state during the uniaxial loading. Careful inspection of these diagrams will show that although all temperature dependent yield surface modification is isotropic (producing concentric yield surfaces), the choice of hardening rule will significantly affect the point of reyield in compression.

CONCLUSION

The theory previously proposed by us has been shown in this report to be adequate in predicting response of many solid media. In addition, it has been shown that certain computationally simplified forms of the theory are correctly in place in the computer code AGGIE I. It has also been shown that the theory may be inadequate in modelling certain physical phenomena. Among these are rate dependence, instability near ultimate strength, finite stress and strain, phase changes, and violation of other assumptions in the theory such as the normality condition. Research is currently underway to incorporate the above additions to the theory.

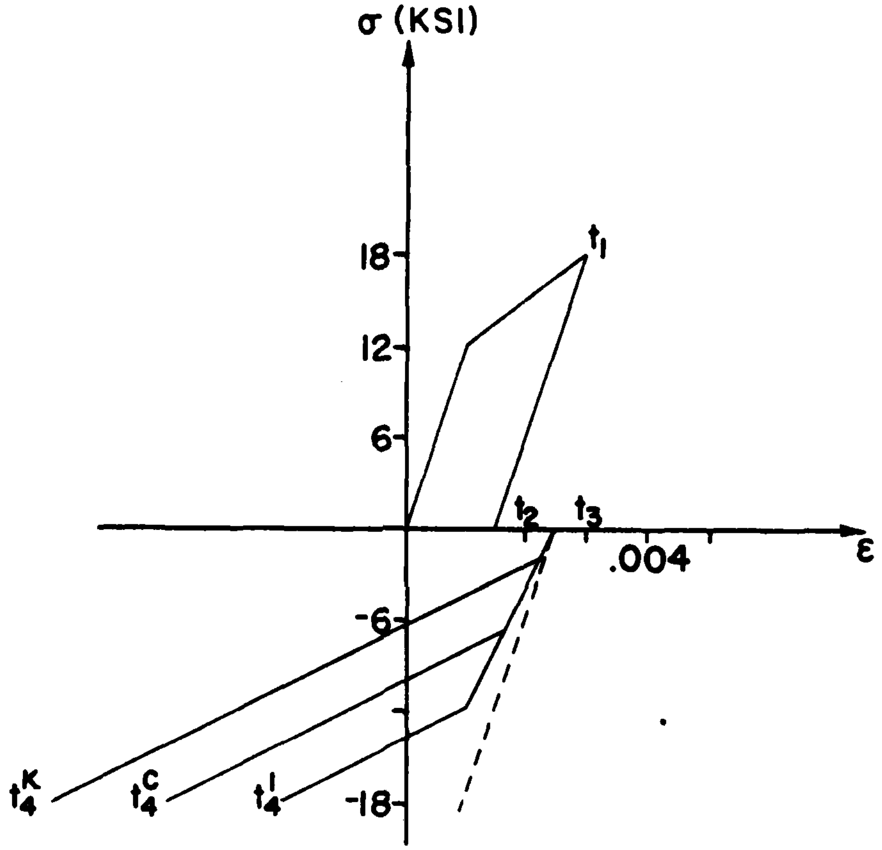

Figure 25. Results for Example Ten

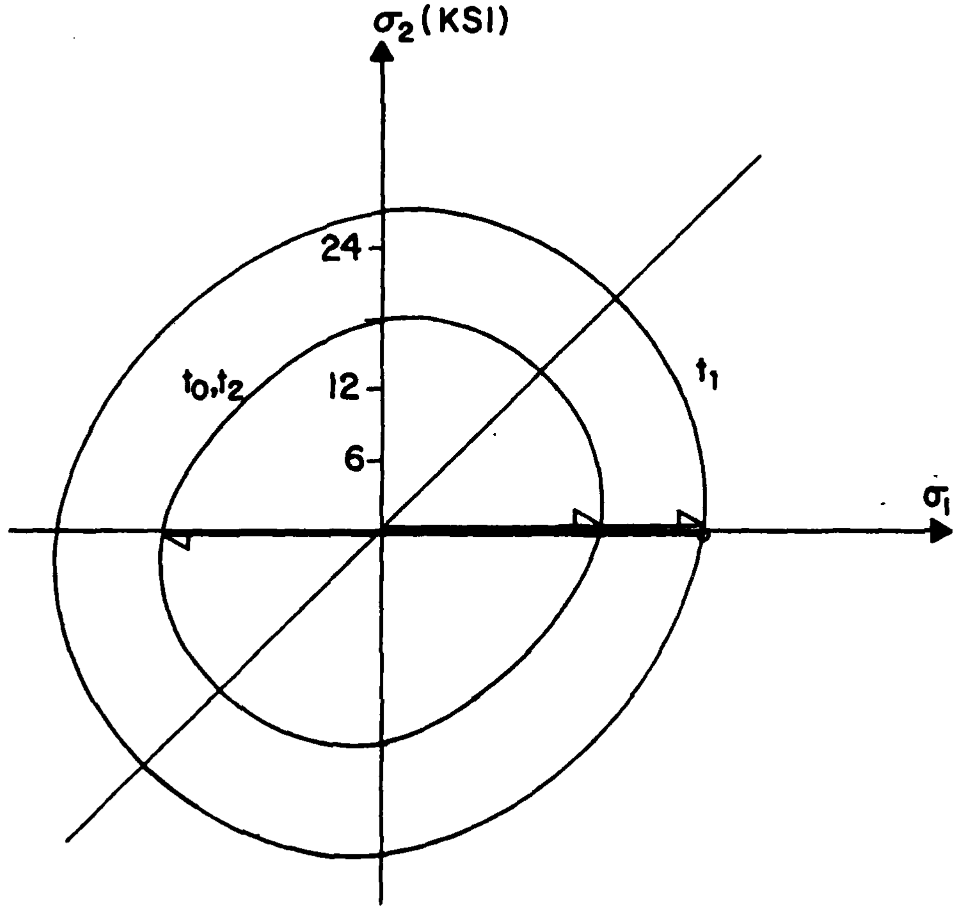

Isotropic Hardening

Figure 26. Nonisothermal Isotropic Hardening of Yield Surface for Example Ten

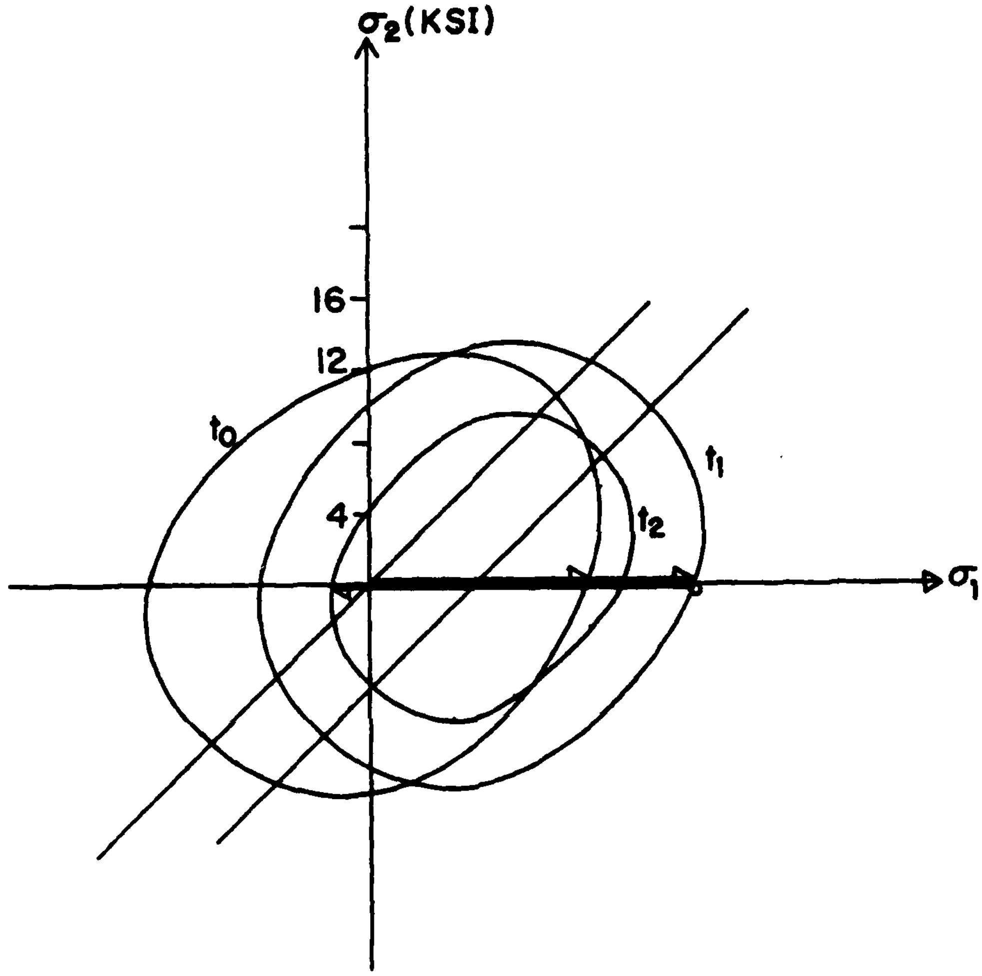

Kinematic Hardening

Figure 27. Nonisothermal Kinematic Hardening
of Yield Surface for Example Ten

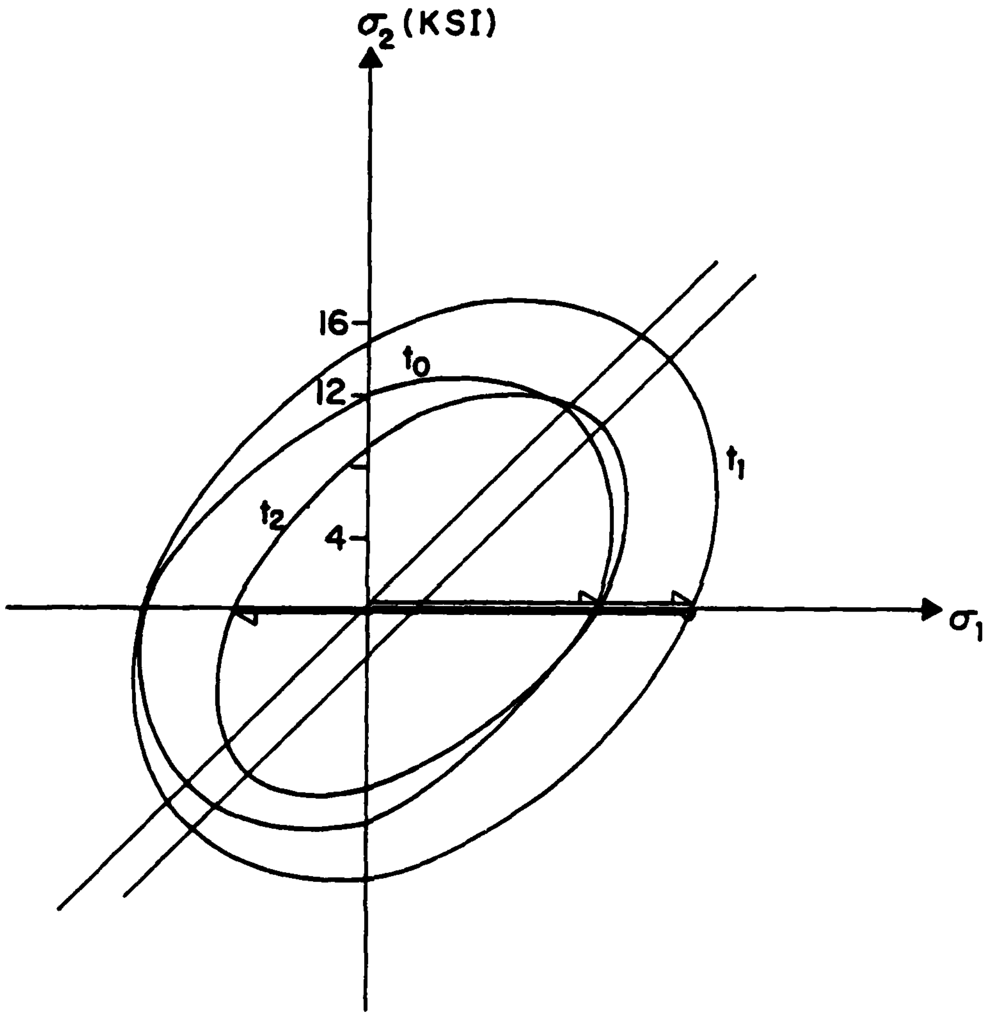

Combined Hardening (β = .5)

Figure 28. Nonisothermal Combined Hardening (β = .5) of Yield Surface for Example Ten

ACKNOWLEDGEMENT

This research was supported by the Office of Naval Research under Contract N00014-76-C-0150.

REFERENCES

1. Allen, D. H., and Haisler, W. E., "The Application of Thermal and Creep Effects to the Combined Isotropic-Kinematic Hardening Model for Inelastic Structural Analysis by the Finite Element Method," Office of Naval Research, No. 3275-79-3, May 1979.

2. Allen, D. H., and Haisler, W. E., "Thermoplastic Analysis Using the Finite Element Code AGGIE I," Office of Naval Research, No. 3275-79-4, December 1979.

3. Snyder, M. D., and Bathe, K. J., "Formulation and Numerical Solution of Thermo-Elastic-Plastic and Creep Problems," Nation Technical Information Service, June 1977.

4. Yamada, Y., and Sakurai, T., "Basic Formulation and a Computer Program for Large Deformation Analysis," Pressure Vessel Technology, Part I, ASME, pp. 341-352, 1977.

5. Haisler, W. E., "AGGIE I, A Finite Element Program for Nonlinear Structural Analysis," Office of Naval Research, No. 3275-77-1, June 1977.

6. Zienkiewicz, O. C., The Finite Element Method in Engineering Science, 3rd edition, McGraw-Hill, Maidenhead, England, 1977.

7. Boley, B. A., and Weiner, J. H., Theory of Thermal Stresses, Wiley, 1960.

8. Tillerson, J. R., and Haisler, W. E., "SAMMSOR II --A Finite Element Program for the Stiffness and Mass Matrices of Shells of Revolution," SC-CR-70-6168, Sandia Laboratories, Alburquerque, New Mexico (also Report 70-18, Aerospace Engineering Department, Texas A&M University), November 1971.

9. Haisler, W. E., and Stricklin, J. A., "SNASOR II --A Finite Element Program for the Static Nonlinear Analysis of Shells of Revolution," SC-CR-71-5155, Sandia Laboratories, Alburquerque, New Mexico (also Report 70-20, Aerospace Engineering Department, Texas A&M University), November 1971.

10. Stone, S. F., "Effects of Material Behavior on the Response of Rapidly Heated Structures," McDonnell Douglas Corporation, No. MDC G8432, Huntington Beach, California, December 1979.

11. Dastidar, G. D., and Ghosh, P., "Stresses and Strains in the Plastic Range in an Annular Disk Due to Steady-State Radial Temperature Variation," International Journal of Mechanical Sciences, Vol. 14, 1972, pp. 501-510.

12. Levy, A., "Development of the PLANS Computer Program for Elastic-Plastic-Creep Analysis of Nuclear Reactor Structural Components," Oak Ridge National Laboratory, Report No. 4485/2RE-567, January 1979.

13. Krieg, R. D., and Duffey, T. A., "Univalve II; A Code to Calculate the Large Deflection Dynamic Response of Beams, Rings, and Plates, And Cylinders," Sandia Corporation, SC-RR-68-303, Sandia Laboratories, Albuquerque, New Mexico, October, 1968.

14. Sanders, D. R., and Haisler, W. E., "An Incremental Form of the Single-Integral Nonlinear Viscoelastic Theory for Elastic-Plastic-Creep Finite Element Analysis," Pressure Vessels and Piping conference, ASME, June 1979.

REPORT DOCUMENTATION PAGE

READ INSTRUCTIONS BEFORE COMPLETING FORM

1. REPORT NUMBER: 3275-80-1	2. GOVT ACCESSION NO.: AD-A087042
3. RECIPIENT'S CATALOG NUMBER	
4. TITLE (and Subtitle): The Prediction of Response of Solids to Thermal Loading using the Finite Element Code AGGIE I	5. TYPE OF REPORT & PERIOD COVERED: Interim
	6. PERFORMING ORG. REPORT NUMBER
7. AUTHOR(s): David H. Allen and Walter E. Haisler	8. CONTRACT OR GRANT NUMBER(s): N00014-76-C-0150
9. PERFORMING ORGANIZATION NAME AND ADDRESS: Department of Aerospace Engineering, Texas A&M University, College Station, Texas 77843	10. PROGRAM ELEMENT, PROJECT, TASK AREA & WORK UNIT NUMBERS: NR064-534
11. CONTROLLING OFFICE NAME AND ADDRESS: Office of Naval Research, Department of the Navy, Arlington, Virginia 22217	12. REPORT DATE: May 30, 1980
	13. NUMBER OF PAGES: 50
14. MONITORING AGENCY NAME & ADDRESS(if different from Controlling Office)	15. SECURITY CLASS. (of this report): Unclassified
	15a. DECLASSIFICATION DOWNGRADING SCHEDULE

16. DISTRIBUTION STATEMENT (of this Report)

Unlimited

17. DISTRIBUTION STATEMENT (of the abstract entered in Block 20, if different from Report)

18. SUPPLEMENTARY NOTES

19. KEY WORDS (Continue on reverse side if necessary and identify by block number)

Finite Element
Thermoelasticity
Thermoplasticity
Creep

20. ABSTRACT (Continue on reverse side if necessary and identify by block number)

In previous work the authors have proposed a theory for predicting the response of elastic-plastic solids subjected to thermal loads. The theory was cast in a finite element framework and has now been placed in the finite element code AGGIE I. In this paper several example problems will be compared to experimental and other theoretical results. It will be shown that the model in its current form is adequate for modelling the response of many solids composed of temperature dependent materials

DATE
FILMED

-8